Received: 23 July 2022 | Revised: 18 April 2023 | Accepted: 23 May 2023

DOI: 10.1002/ppp.2200

RESEARCH ARTICLE

WILEY

Topography and canopy cover influence soil organic carbon composition and distribution across a forested hillslope in the discontinuous permafrost zone

Erin C. Rooney[1,2,3] | Vanessa L. Bailey[2] | Kaizad F. Patel[2] | Alexander Kholodov[4] | Holly Golightly[1] | Rebecca A. Lybrand[1,5]

[1]Department of Crop and Soil Science, Oregon State University, Corvallis, Oregon, USA

[2]Biological Sciences Division, Pacific Northwest National Laboratory, Richland, Washington, USA

[3]Department of Earth and Planetary Sciences, University of Tennessee-Knoxville, Knoxville, Tennessee, USA

[4]Geophysical Institute, University of Alaska Fairbanks, Fairbanks, Alaska, USA

[5]Department of Land, Air, and Water Resources, University of California-Davis, Davis, California, USA

Correspondence
Erin C. Rooney, Biological Sciences Division, Pacific Northwest National Laboratory, 902 Battelle Blvd, Richland, WA, 99354, USA.
Email: erooney2@utk.edu

Funding information
U.S. Department of Energy, Office of Science, Biological and Environmental Research; National Science Foundation (Office of Polar Programs), Grant/Award Number: 2138937

Abstract

Topography and canopy cover influence ground temperature in warming permafrost landscapes, yet soil temperature heterogeneity introduced by mesotopographic slope positions, microtopographic differences in vegetation cover, and the subsequent impact of contrasting temperature conditions on soil organic carbon (SOC) dynamics are understudied. Buffering of permafrost-affected soils against warming air temperatures in boreal forests can reflect surface soil characteristics (e.g., thickness of organic material) as well as the degree and type of canopy cover (e.g., open cover vs. closed cover). Both landscape and soil properties interact to determine meso- and microscale heterogeneity of ground warming. We sampled a hillslope catena transect in a discontinuous permafrost zone near Fairbanks, Alaska, to test the small-scale (1 to 3 m) impacts of slope position and cover type on soil organic matter composition. Mineral active layer samples were collected from backslope, low backslope, and footslope positions at depths spanning 19 to 60 cm. We examined soil mineralogical composition, soil moisture, total carbon and nitrogen content, and organic mat thickness in conjunction with an assessment of SOC composition using Fourier-transform ion cyclotron resonance mass spectrometry (FT-ICR-MS). Soils in the footslope position had a higher relative contribution of lignin-like compounds, whereas backslope soils had more aliphatic and condensed aromatic compounds as determined using FT-ICR-MS. The effect of open versus closed tree canopy cover varied with the slope position. On the backslope, we found higher oxidation of molecules under open cover than closed cover, indicating an effect of warmer soil temperature on decomposition. Little to no effect of the canopy was observed in soils at the footslope position, which we attributed, in part, to the strong impact of soil moisture content in SOC dynamics in the water-gathering footslope position. The thin organic mat under open cover on the backslope position may have contributed to differences in soil temperature and thus SOC oxidation under open and closed canopies. Here, the thinner organic mat did not appear to buffer the underlying soil against warm season air temperatures and thus increased SOC decomposition as indicated by the higher

oxidation of SOC molecules and a lower contribution of simple molecules under open cover than the closed canopy sites. Our findings suggest that the role of canopy cover in SOC dynamics varies as a function of landscape position and soil properties, namely, organic mat thickness and soil moisture. Condition-specific heterogeneity of SOC composition under open and closed canopy cover highlights the protective effect of canopy cover for soils on backslope positions.

KEYWORDS
canopy, carbon, forest, hillslope, permafrost, soil, thaw

1 | INTRODUCTION

The stability of permafrost landscapes and the associated persistence of soil organic carbon (SOC) are disrupted by rapidly warming air temperatures in high latitudes, which contributes to more greenhouse gas emissions to the atmosphere.[1] Vegetation canopy plays a key role in producing summer shade and determines winter snow depths, both of which influence soil temperature, moisture, and freeze–thaw frequency in boreal forests located within the discontinuous permafrost zone.[2–6] The effect of tree canopy can decrease at lower slope positions, with cold and wet conditions favoring smaller trees with less ability to decrease snow thickness on closed canopy soils than larger trees and drier upslope positions.[7] Hillslope processes also contribute to differences in the distribution of SOC and soil properties (i.e., particle size class, mineralogy, and soil moisture) in upslope versus downslope landscape positions.[8] A greater preservation and accumulation of SOC has been reported in lower slope positions (e.g., at the toeslope) than in upslope positions (i.e., backslope, shoulder, and summit).[8–10] Variation in particle size distribution and mineralogy across slope positions may be exacerbated by mass wasting and soil churning that result from cryogenic processes in permafrost environments (i.e., solifluction and cryoturbation), with potential impacts on SOC storage and transformation.[9] Predicting SOC mineralization and release in a warming Arctic requires improving our understanding of the fine-scale heterogeneity of temperature-driven surface soil processes in forested landscapes destabilized by permafrost thaw.

The relationship between permafrost thaw and forest canopy cover is complex and interconnected beyond regulation by soil moisture and temperature.[2,4,11] The manifestation of cryogenic processes (e.g., cryoturbation and frost heave) in forest soils can be initiated by climate and fire impacts, which also influences the molecular structure of SOC in the active layer (seasonally thawed soil depths overlying permafrost). The molecular impact of cryoturbation, the pedogenic mixing of soil material through differential freezing and thawing, was shown in a recent Arctic soil study.[12] Cryoturbated soil contained ~17% of all SOC associated with reactive iron minerals compared with 10% of SOC associated with reactive iron minerals in organic and mineral horizons that did not undergo cryoturbation.[12] Another study examined the chemical characterization of SOC from cryoturbated tundra soils in the Alaskan Arctic and found that SOC from cryoturbated soil horizons showed molecular similarity to surface SOC, likely due to the temperature protection afforded by pedogenic mixing of surface SOC deeper into the profile.[13] In addition, the preservation of the molecular structure of SOC derived from vegetation cover was identified in cryoturbated horizons, resulting in greater bioavailability and thus faster SOC degradation under warming conditions.[13]

Forest canopy cover also has a large influence on ground temperatures apart from fire.[2,4,11] Prior work reported a positive feedback cycle in which canopy loss triggered thaw and the subsequent loss of vegetation.[2,11] Black spruce canopy has been attributed to permafrost protection, given the ability of spruce tree canopies to stabilize permafrost by collecting snow and reducing insulation to the underlying soil during cold months.[4] More information is needed to determine the impact of spruce canopy cover on permafrost hillslopes. Localized differences in ground temperature at the meter level may result in variation in thaw depth and increased winter freeze–thaw cycles, both contributing subsequent impacts to SOC chemistry.[2,3,14,15] The canopy-dependent protection against snowpack insulation and warming is lost when trees die or fail to thrive as observed in occurrences of tree loss, which can increase the susceptibility of soils to increased freeze–thaw cycle frequency depending on the timing and amount of snow precipitation.[3] Freeze–thaw acts as a mechanism in soil biogeochemical transformation by altering mineral–organic matter interactions and affecting microbial cell death and subsequent activity.[16–19] The impact of freeze–thaw and a rise in ground temperatures under insulating snow cover in the open canopy can alter SOC chemistry including decomposition and emissions pathways impacted by moisture conditions and nutrient profiles.[14,15]

Hillslope dynamics also influence soil organic matter (SOM) composition in Arctic landscapes through a combination of erosion–deposition and cryogenic processes or features such as solifluction, cryoturbation, and permafrost protection of SOC.[10,20] An Arctic tundra hillslope experiment investigated molecular scale dissolved organic matter composition in organic and mineral soils across two landscape positions (hillslope and riparian); findings included a greater range of unique SOC-containing molecular formulas in the chemical composition of SOM molecules within the riparian soils than the upper hillslope soils.[21] Permafrost landscapes display a large degree of uncertainty specifically in terms of the size and composition of deep SOC stocks (>3 m) in toeslope positions across the Arctic.[10,22] This uncertainty is the result of insufficient field data and the low

decomposition rates due to high moisture and low temperatures unique to permafrost environments.[10,20,23–25] Understanding the role of canopy-driven temperature variation in SOM composition at SOC-rich lower slope positions can assist in predicting what mechanisms drive mineralization and decomposition as permafrost continues to thaw. Consequently, we predict that canopy-driven temperature dynamics along a hillslope may influence the decomposability and chemical structure of SOC.

Our study aims to investigate how and at what resolution SOC content and composition vary across a forested hillslope as a result of contrasting temperature, moisture, slope, and soil properties. We examined interactions between canopy and hillslope processes in a discontinuous permafrost landscape near Fairbanks, Alaska, that has been prone to rapid thaw. We tested the effect of topographic position and tree canopy cover consisting of black spruce (*Picea mariana*) and white spruce (*Picea glauca*) on SOC chemistry in active layer soils (~20 to 60 cm depths, with permafrost occurring at 60 to 90 cm) across three hillslope positions (backslope, low backslope, and footslope). The term "SOC chemistry" herein refers to the use of Fourier-transform ion cyclotron resonance mass spectrometry (FT-ICR-MS) to examine the composition of the organic matter in the soils. Our interpretations combined FT-ICR-MS analyses with soil morphological observations, soil mineralogy, and total organic carbon and nitrogen elemental data. We hypothesized that there would be greater oxidation of SOC molecules and a lower relative abundance of simple SOC compounds, such as aliphatics, in active layer soils under open cover as a result of warmer subsoil temperatures (soil depths > 5 cm) and increased freeze–thaw cycle frequency compared with soils under closed cover. Similarly, we expected that subsoils under closed cover would reflect the effects of thinner winter snowpack (colder ground temperatures and less frequent freeze–thaw), with less oxidized SOC compounds and a more abundant aliphatic pool. The effect of the canopy was predicted to be weakest for soils in the footslope position where snow accumulation would be thicker under closed cover due to smaller black spruce trees compared with larger white spruce trees on the upslope positions. This work advances the knowledge of the small-scale (1–3 m) heterogeneity of temperature-driven surface processes in forested landscapes containing discontinuous permafrost.

2 | MATERIALS AND METHODS

2.1 | Site description

We established a toposequence, referred to herein as the Y1 transect, in the central part of the Yukon-Tanana terrane near Fairbanks, Alaska (latitude: 64.864103°; longitude: −147.843800°) along a northwest-facing hillslope with an aspect of approximately 330°.[26] The slope ranges from 1° to 7° from footslope to mid-backslope positions.[26] The site has a mean annual temperature of −3°C and a mean annual precipitation of ~500 mm.[27] The area around the University of Alaska Fairbanks is composed of (i) permafrost-free bedrock hills and loess slopes and (ii) permafrost-rich lower hillslope silt and creek-valley silts.[28] We determined that our specific transect occurs in the lower hillslope silt and creek-valley silt deposits based on the geomorphic setting (i.e., silt hillslope) and the presence of permafrost at our site location. The silt and creek-valley silt deposits in the field area are composed of Late Pleistocene–Holocene wind-blown silty deposits of Fairbanks loess that are approximately 15 m thick.[29]

2.1.1 | Soils

Soils in this area are mapped as coarse-silty, mixed, superactive, and subgelic-typic aquiturbels on hills, toeslopes, and footslopes.[30,31] We did not observe evidence for cryoturbation at any of the slope positions that we sampled, although some redox concentrations (oxidized iron) and chromas of two or less were observed in soils under both open and closed cover at the footslope position (see Figure 2 and Figure A1).

Soils were derived from Pleistocene eolian silts (~15 m thick in the Fairbanks area;[28,29]). The degree of slope among the hillslope positions ranged from 5° to 7° at the backslope, 3° at the low backslope, and 1° to 2° at the footslope. Soil profile descriptions, including major horizons with subordinate distinctions, were described and documented during field sampling.[30] Soil particle size distribution was analyzed by the Soil Health Lab at Oregon State University (OSU) using the hydrometer method.[32] Soil pH was measured at a 1:2 soil-to-water ratio on air-dried, sieved, and ground soils using a Hanna HI5522 benchtop meter (HANNA Instruments, USA) by OSU's Soil Health Lab.

2.1.2 | Vegetation

White spruce dominates the overstory on the backslope position, with sparse birch being observed. Black spruce is the dominant overstory at the low backslope position, with black spruce and larch being most prominent in the footslope position. Shrubs at all slope positions were dominated by diamond-leaf willow (Table 1).

2.2 | Sampling

We selected three slope positions along the toposequence to compare how the effect of cover type on soil temperature and SOM differed depending on the slope position and associated soil moisture, texture, and SOM composition. We focused specifically on backslope, low backslope, and footslope positions to maintain consistency between open and closed canopy plots; the summit and shoulder positions contained cryogenic surface features (patterned) that impacted soil temperature distribution. We examined a total of 18 soil pits, where 6 soil pits were described and sampled in each of the three slope positions. Within each slope position, three pits were excavated beneath the closed canopy and three under the open canopy

TABLE 1 Geobotanical structure of the catena via field observations and descriptions

	Trees	Shrubs	Understory
Backslope	White spruce (*Picea glauca*) and birch (*Betula papyrifera*)	Diamond-leaf willow (*Salix planiofolia*)	Feather moss (Hypnales), dogwood (*Cornus florida* L.), grasses, and sedges
Low backslope	Black spruce (*Picea mariana*)	Diamond-leaf willow (*S. planiofolia*)	Sphagnum moss and labrador tea (*Rhdodendron groenlandicum*)
Footslope	Black spruce (*P. mariana*) and larch (*Larix laricinia*)	Diamond-leaf willow (*S. planiofolia*)	Sphagnum moss, labrador tea (*R. groenlandicum*), cotton grass (*Eriophorum angustofolium*), and dwarf birch (*Betula nana*)

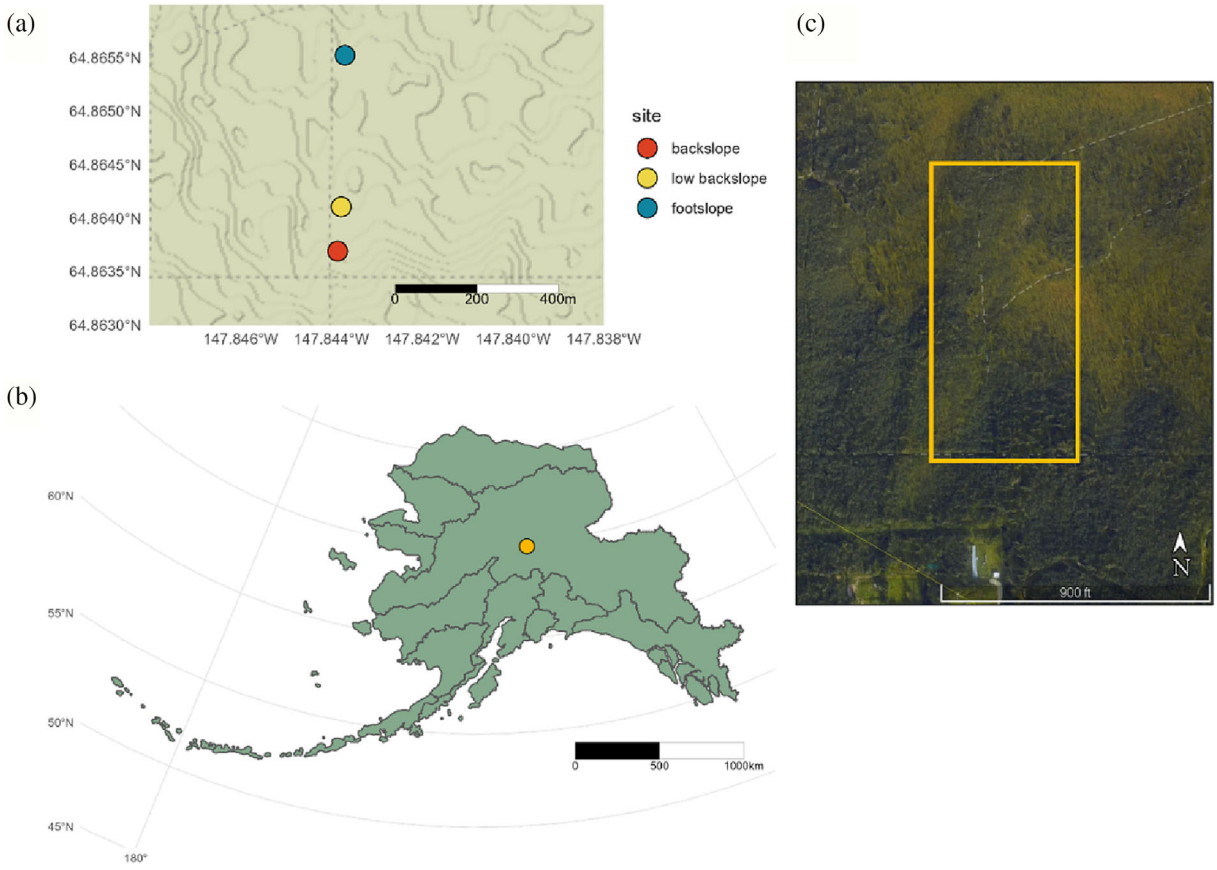

FIGURE 1 (A) Site map of the catena in Fairbanks, Alaska, depicting slope positions (footslope, low backslope, and backslope) (citation: ggmap); (B) site map depicting Fairbanks site location within Alaska (derived from Kibele and Clark, 2018[35]); (C) terrain view of the transect (gold box depicts the transect area) provided by Google Earth (2023, Maxar Technologies)

(Figures 1A and 1B). Closed cover was defined as a site that is in close proximity (<1 m) to one or more trees, and open cover was defined as a site located at least 3 m from nearby trees with little to no canopy coverage (<∼10%) above each sampling location. Diameter at breast height (DBH) was also recorded for three random trees at each slope position.[33,34] DBH was approximately 1.45 m above the ground surface.

Soil temperatures at the surface (5 cm) and subsurface (75 cm) were recorded at the backslope position via a borehole from 2020 to 2021. Soil temperature sensors (TMC-HD, Onset Computer Inc., USA) were placed at 5 and 75 cm, with temperatures recorded every 6 h. Freeze–thaw cycles were quantified using the method adapted and modified from Rooney et al. (2022)[36] using the FTCQuant R Package.[37] The total number of freeze–thaw cycles was calculated for the period of May 2020 to September 2021 when data sets were complete for both open and closed cover soils at depths of 5 and 75 cm. Due to the large time increments (6 h), we defined a freeze–thaw cycle as any temperature fluctuations above and below 0°C across two timesteps (for 6 h above and 6 h below 0°C). Freeze–thaw counts provide general information about temperature fluctuations in surface and deeper soils under open and closed cover at a single location in the backslope site.

Soil sampling was focused on the collection of active layer mineral soil samples to address our experimental objective to investigate how SOC content and composition varied across a forested hillslope. One to three active layer mineral soil horizons were sampled between ~20 and 60 cm for each soil profile and pooled within each soil profile for statistical analysis (for a total of three replicates per each slope position and cover type combination). Samples were pooled by soil profile to address the main research question comparing soil properties and SOM chemistry across hillslope positions and cover types. Samples were maintained under frozen conditions (<0°C) and transported to Oregon State University for analysis and preservation. Samples were maintained at −20°C in a laboratory freezer.

2.3 | Fourier-transform ion cyclotron resonance mass spectrometry

Soils were subsampled by the horizon and analyzed for high-resolution SOC characterization using water extractions at the Pacific Northwest National Laboratory's Environmental Molecular Sciences Laboratory (Richland, WA, USA). FT-ICR-MS analysis was performed on fresh, field-moist soil samples. Samples were prepared as water-extractable organic carbon (WEOC) extracts and analyzed via automated direct infusion on a 21 T FT-ICR mass spectrometer. Briefly, 300 mg of soil was weighed into 2 ml MicroSolv vials, with 1 ml of MilliQ added. Vials were shaken on a ThermoMixer for 2 h at 2,000 rpm at room temperature and then filtered through 0.45 µm Hydrophilic PTFE filters for WEOC extracts.

An extensive overview of the FT-ICR-MS measurement, analysis, and data visualization approach is provided in the appended materials (see Appendix A.1). Samples were randomized for analysis after ionization through dilution with methanol (MeOH) at a ratio of 1:2 (sample:MeOH). For each sample, 144 individual scans were averaged to improve the overall abundance of ions detected. Bruker DataAnalysis (signal-to-noise ratio of 7) was used for peak selection and calibration. Formulas were assigned using the in-house Formularity software, with further data processing performed with the fticrrr R package.[38] All peaks were analyzed on a presence/absence basis, and only peaks occurring in two-thirds of replicates were considered to be present. Only carbon-containing formulas between 200 and 900 *m/z* mass were included.

Briefly, we compared *total peaks* across canopy cover types and hillslope positions and peaks *unique* to open cover and those *unique* to closed cover to identify chemical differences. Ratios of hydrogen-to-carbon (H/C) and oxygen-to-carbon (O/C) are depicted on van Krevelen plots, with different regions being associated with specific compound classes (depicted in Figure 8). We used the nominal oxidation state of carbon (NOSC) to analyze the thermodynamic favorability of compounds and potential microbial oxidation. The association between NOSC and thermodynamics assumes oxic conditions and the use of oxygen as the dominant terminal electron acceptor, which is reflected in the established relationship between Gibbs Free Energy and NOSC.[39,40]

2.4 | X-ray diffraction

Soils were air-dried, sieved to <2 mm, and ground to <50 µm. Subsamples were analyzed at the Environmental Molecular Sciences Laboratory (Pacific Northwest National Laboratory). Powder X-ray diffraction (XRD) patterns were collected using a Rigaku SmartLab SE diffractometer (Rigaku Corporation, Japan) on powders packed into zero-background well holders. The diffractometer used Bragg–Brentano geometry with a Cu X-ray source (λ = 1.5418 Å), a variable divergence slit, and a high-speed D/teX Ultra 250 1D detector. Patterns were collected between 2 and 100°2θ at intervals of 0.01°2θ, scanning at 2°2θ/min. Details on the quantification method are available in the appended materials (see Appendix A.2).

2.5 | Total carbon and nitrogen

Samples were air-dried, sieved, and ground prior to analysis for the total nitrogen and carbon on a Vario EL Cube Elemental Analyzer (Elementar Analysensysteme GmbH, Langenselbold, Germany). Homogenized samples were weighed and sealed into tin boats (Elemental Microanalysis Ltd., Devon, United Kingdom). Samples were combusted at 1,150°C in the presence of oxygen. The signals for nitrogen and carbon were measured using a thermal conductivity detector. The detector response was calibrated using aspartic acid and checked using a soil reference material. SOM percentage was also measured for reference via loss on ignition by Oregon State University's Soil Health Lab (16 h at 385°C on a Thermolyne F-A1730 oven).

2.6 | Statistics

Statistical tests were performed across pits (with individual depth data grouped within each sampled soil profile) (Tables A1–A3 and A7–A9). For individual depth data, all SOM datasets are shown across individual horizons in Tables A4–A6 and A9–A11. FT-ICR-MS data were analyzed using univariate linear mixed-effects (LME) models and principal components analysis (PCA) to test the effect of slope position (backslope, low backslope, and footslope) and cover type (closed and open) and their interactions on the relative abundance of compound classes and the NOSC. XRD mineral abundances were tested using ANOVAs, with HSD tests being used to determine statistical differences across the three hillslope positions. Tree diameter (DBH) was tested with ANOVA and Tukey HSD. The effect of cover type and hillslope position on soil properties (pH, SOM%, total carbon [TC], total nitrogen [TN], gravimetric water content, carbon-to-nitrogen [C:N] ratio, and organic mat thickness) was tested via ANOVA with Tukey HSD tests and supplemented with LME (horizonation as a random effect) to investigate the effects of cover type within each individual slope position. Statistical significance for LME, ANOVA, and Tukey HSD was determined at $\alpha = 0.05$. Data analysis and visualization were performed using R version 4.0.1 (2020-06-06) with RStudio version 1.4.1106.[41] Data processing and analysis were conducted using dplyr

v1.0.1[42] and vegan v2.5–6[43] packages. Data visualization was performed with ggplot2 v3.3.2,[44] and map visualization was conducted via ggmap.[45] The Algorithms for Quantitative Pedology suite of R packages (aqp, soilDB, and sharpshootR) were used to compile and visualize soil horizons and soil color data. All data and scripts are available at https://github.com/Erin-Rooney/Y1_fairbanks and archived and searchable at https://search.emsl.pnnl.gov (Project ID #50267).

3 | RESULTS

3.1 | Soil temperature and tree diameter

Temperatures differed between open and closed canopies where surface and subsurface soils under open cover were generally warmer than soils under closed cover. Average surface soil temperatures during the winter were ~−5°C under open cover compared with ~−12°C under closed cover. In contrast, summer temperatures were slightly higher under closed cover in surface soils: ~10.5°C under open cover compared with ~12°C under closed cover (Figure 2). In the subsurface depth (75 cm), winter temperatures were ~−1°C under open cover and −1.5°C under closed cover. In summer, subsurface temperatures were −0.1°C under open cover and −0.2°C under closed cover. Warmer temperatures under open cover did not result in increased freeze–thaw cycle frequency in surface soils. Instead, the surface soils under closed cover experienced a greater frequency of freeze–thaw events both in spring and in fall (Figure 2). Under closed cover, the surface depth (5 cm) underwent 47 freeze–thaw cycles, whereas the deeper soil depth (75 cm) did not undergo any freeze–thaw cycle. By contrast, open cover soils underwent six freeze–thaw cycles at both 5 and 75 cm during the same time period (between May 2020 and September 2021). In contrast, warmer temperatures under open cover did result in slightly higher freeze–thaw cycle frequency in subsurface soils than under closed cover.

Tree canopy characteristics varied with slope position: the footslope was dominated by black spruce trees, whereas both backslope and low backslope positions were dominated by white spruce trees. Tree diameters varied with the slope position, where the low backslope position contained trees with the largest average DBH, followed by backslope, with the smallest DBH at the footslope position (ANOVA, $p < 0.05$; Figure 3). Differences in the tree diameter and overall size of the canopy may have resulted in variations in snow cover across slope positions under closed cover.

3.2 | Soil morphology and taxonomy

3.2.1 | Variation in soil morphology and organic mat thickness along the toposequence

Organic surface soils

All slope positions and cover types had soils with peat and mucky peat O horizons overlying A, Bw, or C horizons, and similar soil

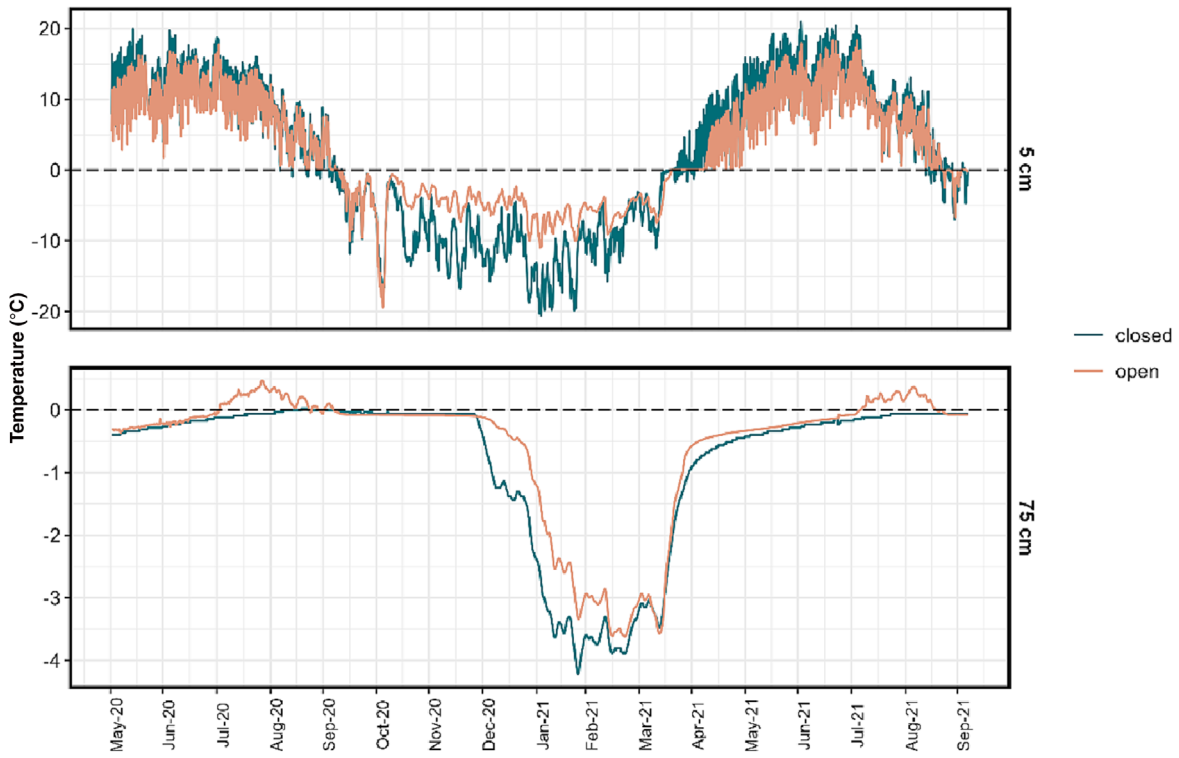

FIGURE 2 Temperature fluctuations at 5 cm (upper panel) and 75 cm (lower panel). Temperature measured from open cover (tan) and closed cover (green) at the research area between the backslope and low backslope positions from May 2020 to September 2021. The dashed black line indicates 0°C

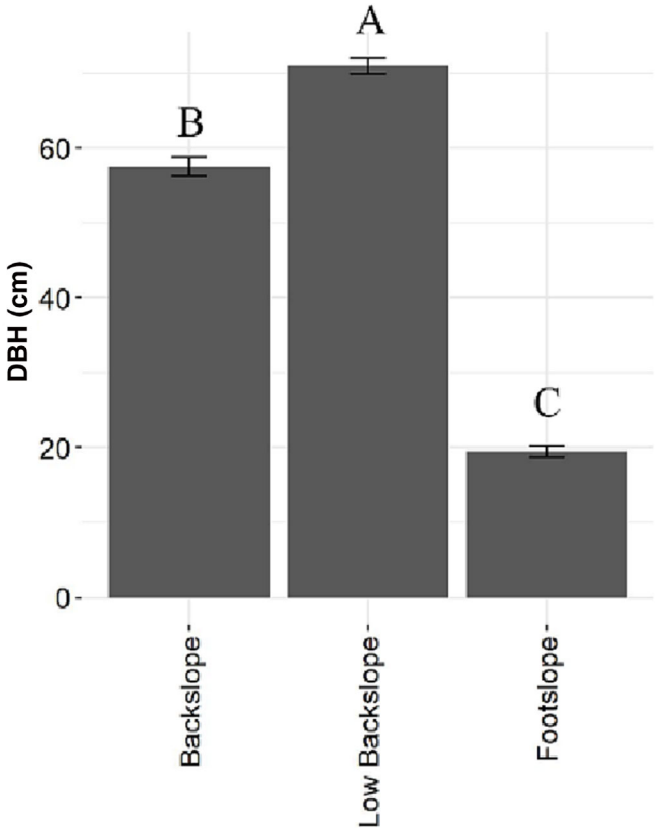

FIGURE 3 Tree trunk diameters (diameter at ~1.45 m height). Statistical comparisons are made between slope positions (backslope, low backslope, and footslope); $p < 0.05$. All values are in centimeters

morphological properties were observed throughout sites, with some variation in organic matter content and moisture conditions (Figure 4 and Table 2). Organic mat thickness also varied by slope position, with soils in the footslope position presenting thicker organic mat depths of 27.7 to 36 cm compared with 18 to 25.3 cm depth ranges in upslope soils (ANOVA, $F = 14.5$, $p = 0.0006$). The interaction of slope position with cover type (ANOVA, $F = 7.5$, $p = 0.008$) had an effect on organic mat thickness and no effect on cover type alone ($p = 0.5$) (Table 2). Soils under open cover had greater organic mat thicknesses than under closed canopies on the low backslope and footslope. Soils under open cover had organic mat thicknesses of 21 to 29 cm on the low backslope and 33 to 42 cm on the footslope, yet organic mats were thinner in soils under open cover at the backslope position (16 to 19 cm) than those under closed cover on the backslope (22 to 28 cm).

Mineral subsurface soils

Subsurface mineral horizons showed higher organic matter percentages in the footslope and low backslope positions, with averages spanning ~8% to ~3.85%, respectively, in comparison to ~2.5% in the backslope position (organic matter percentage determined via loss on ignition). The soil texture for all soils was silt loam, with the exception of loam soil textures present under closed cover at the backslope position (Table A1). Soil pH differed by the slope position ($p < 0.001$) but not by the cover type. Soil pH was highest on the backslope (7.5), second highest on the low backslope (6.9), and lowest on the footslope (6.2), as indicated by a Tukey HSD test (Table 2). Soil pH did not vary significantly by the cover type (Table 2).

TC and TN contents were greater in soils from the footslope position compared with the backslope position (ANOVA, $p < 0.05$; Tables 2 and A4–A6). Soils on the backslope and low backslope had the lowest SOM content under open cover (1.5 ± 0.2% on the backslope and 2.8 ± 0.6% on the low backslope) versus 10.9 ± 5.4% on the footslope, with closed cover soils following a similar pattern (Table 2). C:N ratio varied across slope positions (ANOVA, $F = 7.875$, $p = 0.0006$), with the highest C:N ratio of 21 in soils from the footslope position according to a Tukey HSD test compared with 19 in soils from both low backslope and backslope positions. There was an interaction of slope position and cover type with the C:N ratio (ANOVA, $F = 6.609$, $p = 0.002$), although cover type on its own showed no effect.

Gravimetric water also varied across slope positions (ANOVA, $F = 9.841$, $p = 0.0004$). Soils in the footslope position contained the highest-moisture contents (37.5% to 42.4%), whereas backslope and low backslope soils had mean moisture contents of 20.8% to 26.5%. However, the soil moisture content did not differ between open and closed cover types (Table 2). Gleyed colors were observed in backslope, low backslope, and footslope soils (i.e., 2.5Y 4/1, 10YR 3/1, and 2.5Y 3/2, respectively). Only footslope soils contained oxidized iron and saturated conditions (Figure A1 and Table 2). The absence of other redox features at the backslope and low backslope positions may indicate that the soil color was lithogenic (derived from loess silts) rather than reduced matrix soil. Only footslope soils had Bg soil horizons (i.e., 2.5Y 3/2) and contained oxidized iron.

3.2.2 | Soil taxonomic classifications

All soils were classified as Cryosols according to the World Reference Base,[46] given that cryic horizons (perennially frozen organic or mineral soil) occurred between ~60 and 90 cm at all slope positions. All soils contained folic horizons (unsaturated organic layers) in the upper 20 cm (Figure A2; 4.[46] The soils were also classified as Gelisols with folistic diagnostic epipedons using the US Soil Taxonomy System. Organic horizons were present at the soil surface but did not extend to 40 cm, and cryoturbation was not observed. This evidence supports the Great Group taxonomic naming of these soils as Historthels.[30] Although some redoximorphic features were noted on the footslope, cambic horizons were identified throughout. We observed weakly developed Bw horizons beneath the organic horizons that displayed the requirements for cambic horizons based on the expression of organic matter accumulation in the mineral soil horizons. The soils were classified as Gelisols with folistic diagnostic epipedons using the US Soil Taxonomy System. This evidence supports the Great Group taxonomic naming of these soils as Historthels.[30]

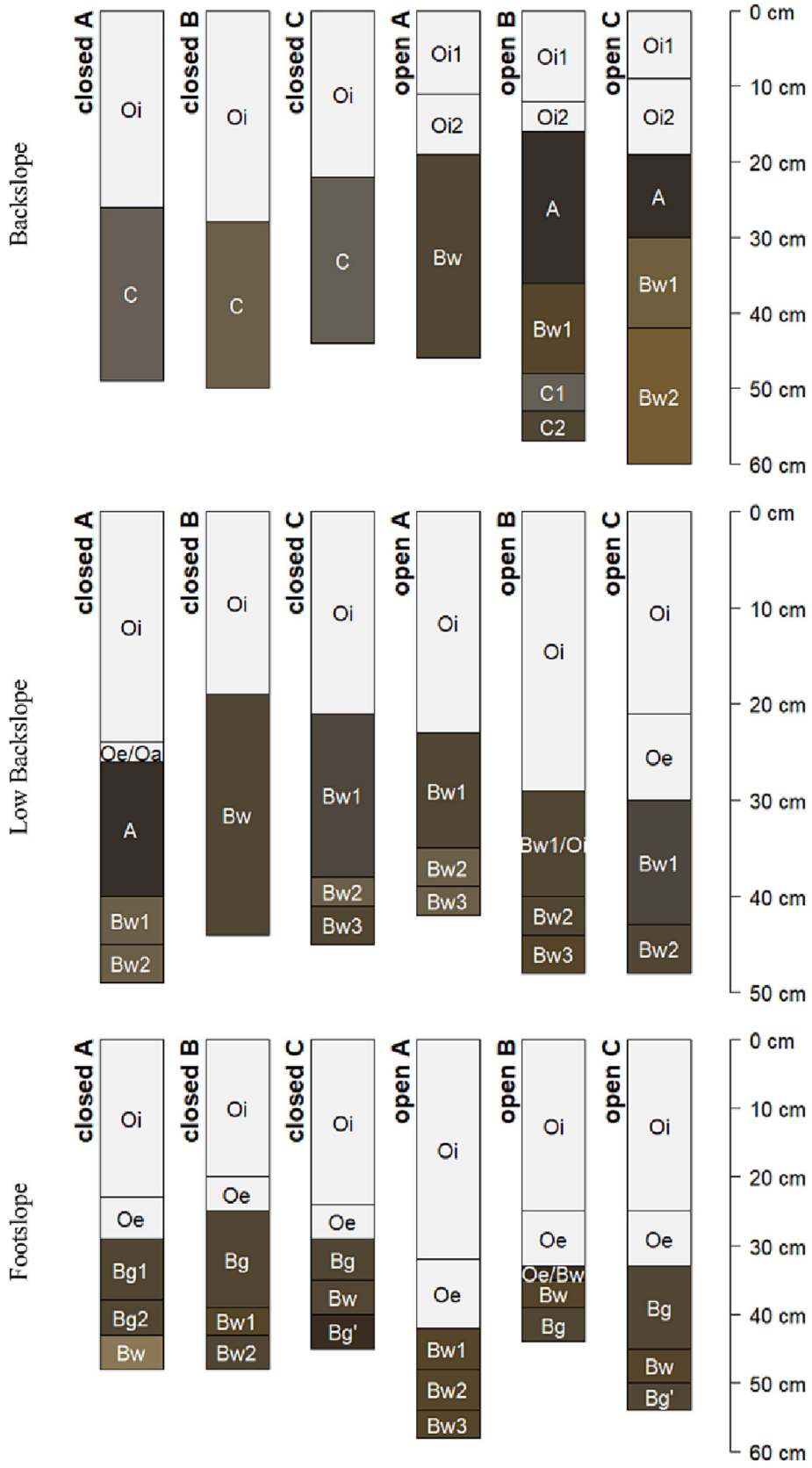

FIGURE 4 Soil profile morphology and measured Munsell colors of each mineral soil horizon within the study. Mineral soils are described morphologically, sampled, and analyzed. Organic horizons are described morphologically, and horizonation is provided

TABLE 2 Soil properties including soil moisture, TC, TN, C:N ratio, SOM, organic mat thickness, and pH

	Gravimetric water (%)	TC (%)	TN (%)	C:N ratio	SOM (%)	Organic mat thickness (cm)	pH
Backslope							
Closed	22.7 ± 1.8	1.01 ± 0.14	0.05 ± 0.01	19	3.5 ± 0.8	22 to 28	7.35
Open	20.8 ± 1.2	0.44 ± 0.05	0.03 ± 0.00	16	1.5 ± 0.2	16 to 19	7.66
Low backslope							
Closed	26.5 ± 3.9	1.43 ± 0.29	0.08 ± 0.02	17	4.9 ± 2.8	19 to 26	6.86
Open	23.4 ± 1.1	1.82 ± 0.32	0.10 ± 0.02	19	2.8 ± 0.6	21 to 29	6.98
Footslope							
Closed	37.5 ± 3.7	2.54 ± 0.35	0.13 ± 0.02	19	5.1 ± 1	25 to 29	6.27
Open	42.4 ± 7.9	4.43 ± 0.97	0.21 ± 0.04	21	10.9 ± 5.4	33 to 42	6.04

Note. TC was determined through elemental analysis, whereas SOM was measured by LOI. Soil properties varied by the slope position. The soil in the footslope position was wetter, presented greater TC and TN percentages, and was more acidic than that in upslope positions (ANOVA, $p < 0.05$). We sampled each soil horizon within the mineral active layer. Data were pooled across all depths within each replicate and then averaged across each cover type and slope position combination. The standard error is reported. Individual horizon data sets are presented in Tables A4–A6, and significant effects are shown in Table A2.

Abbreviations: LOI, loss on ignition; SOM, soil organic matter; TC, total carbon; TN, total nitrogen.

3.3 | Soil mineralogical properties

The analyses of soil mineralogical abundance and composition indicated that the mineral composition of the soils was consistent across the cover type and slope position, with only minor differences being found in abundance (Table A3 and Figures A3–A6). Overall, the mineralogical assemblage for the soils in the field area was predominately composed of quartz, anorthite, albite, and mica, with more minor amounts of chlorite, microcline, hornblende, and ankerite. We note that the XRD diffractogram patterns show a carbonate mineral with a strong peak at 2.89 Å consistent with Ca (Mg, Fe, Mn)CO_3. The best match was found for the Fe-containing mineral ankerite although its low abundance means that identification cannot be made with certainty compared with related minerals such as dolomite. The footslope position had a higher percentage of muscovite mica (13% to 14%) and chlorite (6% to 8%) compared with respective values of 9% to 10% for muscovite and 5% to 6% for chlorite in both the low backslope position and backslope positions (ANOVA, $p < 0.05$; Table A3). Quartz and ankerite values were also lowest for soils in the footslope position, with respective percentages of 40% to 41% and 0.29% to 0.34%. Low backslope soils contained 42% to 44% quartz and 0.55% to 0.8% ankerite versus backslope soils containing 43% to 46% quartz and 0.58% to 0.84% ankerite (ANOVA, $p < 0.05$).

3.4 | SOC chemistry

FT-ICR-MS-resolved carbon composition varied by hillslope position and cover type (Figures 5 and 6). A PCA showed an effect of slope position, with the largest separation occurring between footslope and backslope positions. SOC composition at the footslope position was strongly influenced by lignin-like compounds, whereas backslope soils had more aliphatic and condensed aromatic compounds (Figure 5). The total number of FT-ICR-MS-resolved peaks varied with slope position and cover type (Table 3 and Figure 6). Peak richness differed by slope position. The backslope position had <3,000 peaks under both open and closed cover, whereas the low backslope and footslope positions had >6,000 peaks (and up to 10,000 peaks under closed cover on the footslope) (Table 3 and Figure 6). The overall O/C and H/C ratios were comparable across all slope positions and cover types despite differences in peak count (Figure 6 and Table 3).

In addition to the *total* identified FT-ICR-MS-resolved peaks within all treatments, we investigated differences in peaks *unique* to cover type and slope position. We found that slope position and cover type affected the degree of oxidation, as represented using NOSC, of unique peaks both separately and in combination (ANOVA, $p < 0.005$). A Tukey HSD test showed that NOSC was lower in FT-ICR-MS-resolved peaks unique to soils from the footslope position compared with peaks unique to the backslope and low backslope positions (Figure 8A).

We detected a higher relative abundance of lignin-like compounds in soils from the footslope than from the backslope position (∼8% higher under closed and 12% higher under open; ANOVA, $p < 0.05$) (Figure 7). The relative abundance of aliphatics followed a similar trend by decreasing from ∼35%–39% in backslope soils to ∼28%–30% in soils from the footslope (Figure 7 and Table A7; $p < 0.05$).

The degree of oxidation and SOC composition varied by topographic position and between soils under open and closed canopy cover (Figures 7 and 8). Our analysis of unique peaks revealed that NOSC was higher under open cover than under closed cover on the backslope, but the opposite was observed for low backslope soils where NOSC was higher under closed cover than under open cover (ANOVA, HSD test, $p < 0.05$; Figure 8A). There was no difference in NOSC under open or closed cover in soils from the footslope position. In the associated van Krevelen diagram, there is a notable separation between cover types for high O/C ratio (>0.75 O/C) compounds at

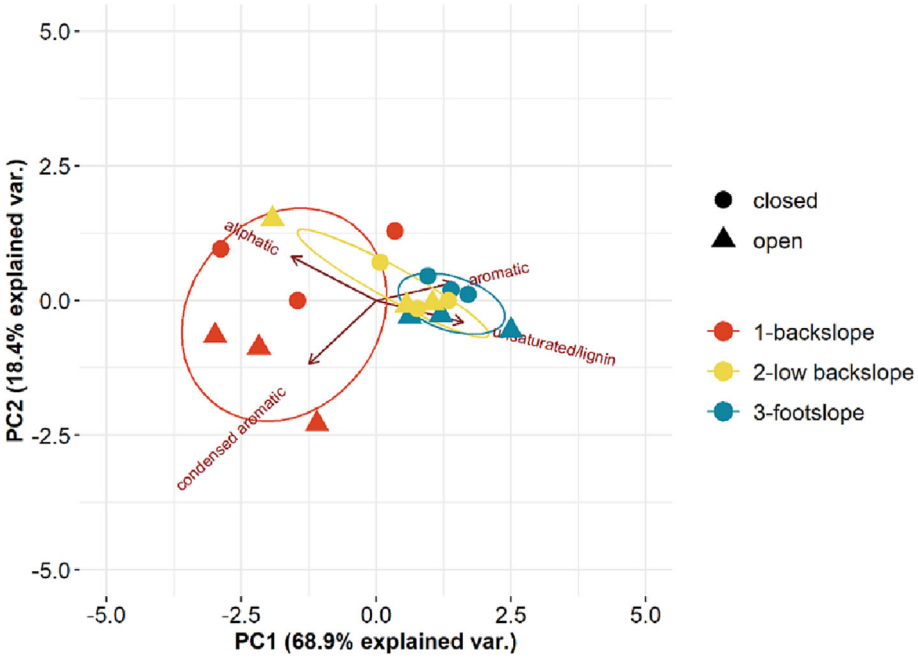

FIGURE 5 Principal component analysis biplot of Fourier-transform ion cyclotron resonance mass spectrometry data showing the separation by hillslope position for both closed (circles) and open (triangle). Ellipses represent 95% confidence intervals

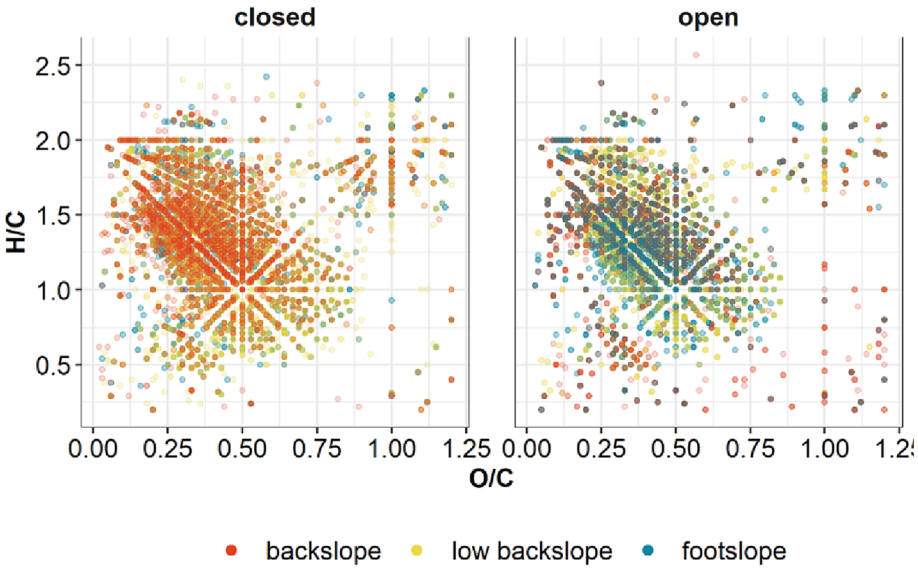

FIGURE 6 Van Krevelen plots showing organic compounds by slope position and cover type. Molecules are plotted as functions of their H/C and O/C ratios

TABLE 3 Total FT-ICR-MS-resolved peaks by treatment

	Open	Closed
Backslope	2,768	2,296
Low backslope	6,238	7,365
Footslope	6,965	10,041

Note. Peaks were calculated across all replicates.
Abbreviation: FT-ICR-MS, Fourier-transform ion cyclotron resonance mass spectrometry.

the backslope position. The separation in high O/C molecules by cover type occurs at 1.5 H/C (the delineation between aliphatic and lignin-like compounds) (Figure 8B). Specifically, the van Krevelen diagram showed lignin-like, aromatic, and condensed aromatic molecules with high O/C (> 0.75 O/C) ratios under open cover but not closed cover on the backslope. This delineation by cover type is not observed in high O/C molecules in low backslope and footslope soils. High O/C ratio aliphatics are shown under closed cover at all hillslope positions.

SOC compounds in backslope soils were more oxidized under open cover, with aromatics and lignin-like compounds showing increased oxidization and a higher relative abundance of condensed aromatics compared with closed cover. SOC was less oxidized under open cover in the low backslope position, with both aliphatic and lignin-like compounds showing decreased oxidization and lower relative abundance of aromatics compared with closed cover. A NOSC breakdown by class explores this finding further, showing diverging oxidation states across compound classes in unique peaks associated with open and closed cover types at all slope positions (Figure A7).

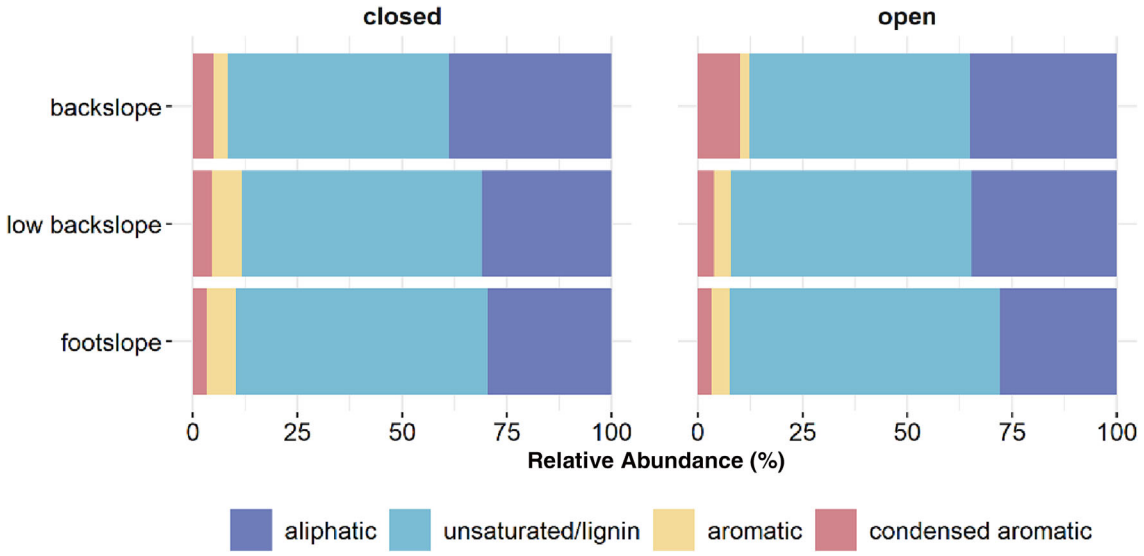

FIGURE 7 Relative abundances of carbon compound classes with comparisons between slope positions. Differences are determined at significance 0.05. Statistical comparisons are made between slope positions within cover types. All values are in percentages (%)

FIGURE 8 Backslope soils under open cover had higher NOSC, with lignin-like, condensed aromatic, and aromatic molecules showing greater oxidation. Low backslope soils under open cover had lower NOSC. (A) NOSC of compounds unique to each cover type by slope position. (B) Van Krevelen plot showing organic compounds unique to each cover type by slope position. Molecules are plotted as functions of their H/C and O/C ratios. Ellipses represent 95% confidence intervals

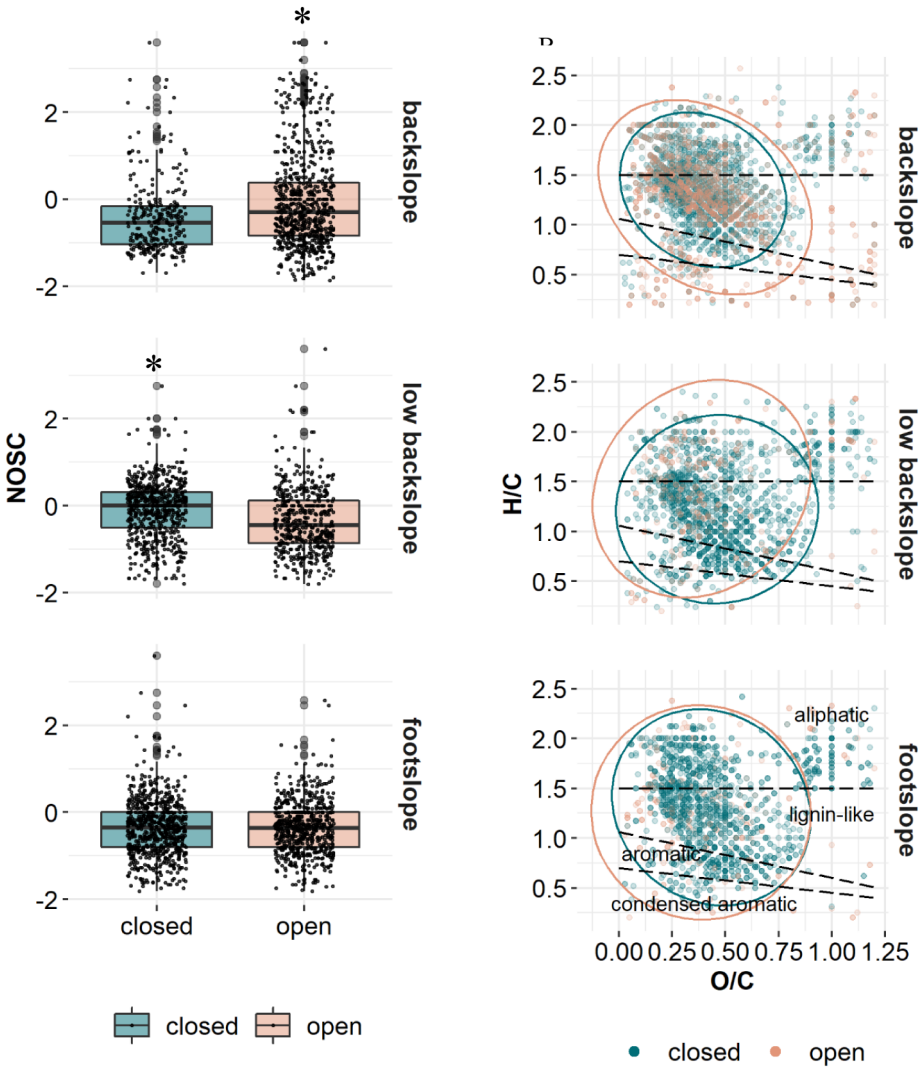

The more complex molecules (aromatics and lignin-like compounds) were more oxidized under the open canopy than under the closed canopy in backslope soils, as indicated by the van Krevelen diagram (Figure 7) and further supported by the NOSC breakdown by carbon class (Figure A7). Notably, we made a contrasting observation on the low backslope where both simple and complex (aliphatic and lignin-like, respectively) compounds were less oxidized under open cover than under closed cover. Aromatics were more oxidized under open cover, whereas aliphatics were less oxidized in soils from the footslope position (Figure A7).

We also found differences in the relative abundance of carbon classes across *total* FT-ICR-MS-detected peaks between open and closed cover at each slope position (Table A8). The relative abundance of condensed aromatics was twice as high under open cover (~10%) as under closed cover (~5%) on the backslope position. Conversely, the relative abundance of aromatics was lower under open cover (~4%) than under closed cover (~7.2%) on the low backslope position. The relative abundance of lignin-like compounds was higher under open cover (~64.3%) than under closed cover (~60.2%) in soils from the footslope position (Tables A9–A11).

4 | DISCUSSION

4.1 | Organic mat thickness and soil temperature

We found that the effect of open versus closed cover on carbon chemistry was either heightened or reduced depending on the slope position on the sampled northwest-facing hillslope investigated during our study (Figures 7–9). Our findings presented strong evidence for meter-scale differences (~1 to 3 m) in FT-ICR-MS-resolved SOC chemistry, with an effect of the cover type observed at the backslope and low backslope positions, whereas little to no effect was seen at the footslope position. The diverging observations for the carbon dynamics are notable, given that the data coincide with DBH results that found statistically larger tree trunk diameters at the low backslope position than at the backslope position (Figure 3). We expected that the larger tree canopy would have resulted in more pronounced differences in ground temperature at the low backslope as snow cover would be more effectively held in the larger canopy. However, contrasting organic mat thicknesses of 16 to 19 cm in soils under open cover on the backslope and 21 to 29 cm in soils under open cover on the low backslope position may

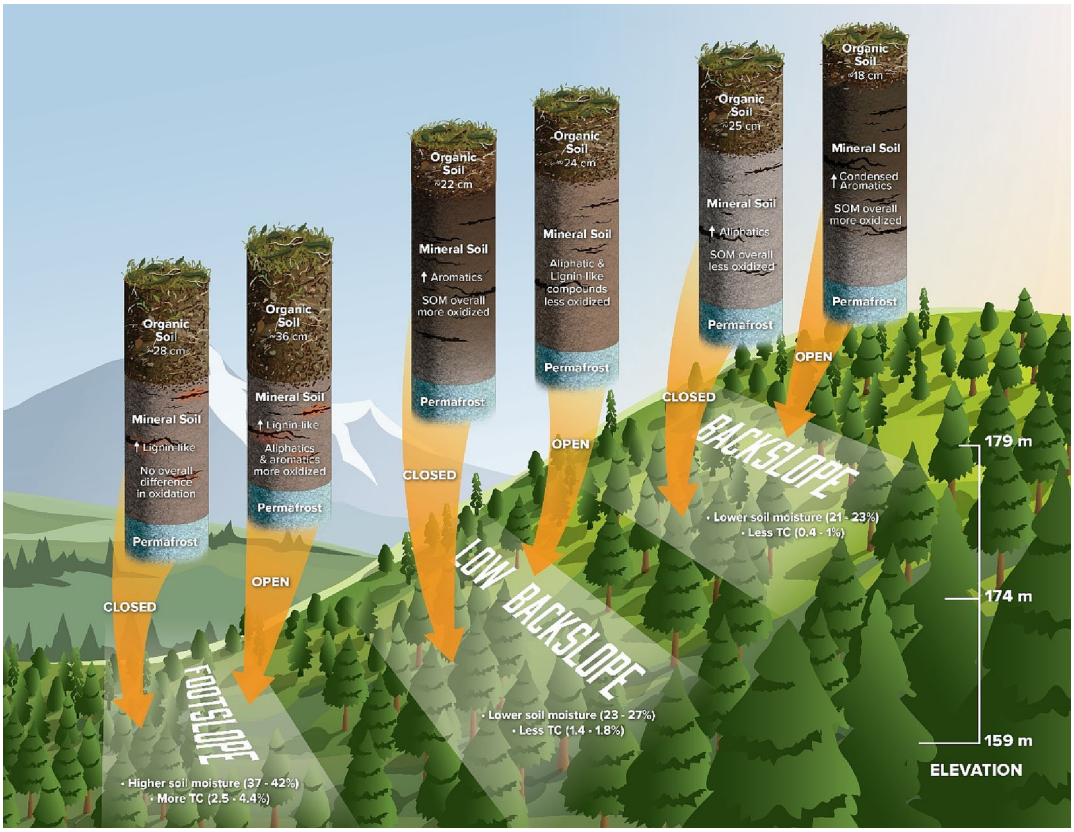

FIGURE 9 Belowground differences in soil organic carbon composition and soil morphology across hillslope positions and cover types. Soils showed evidence for higher oxidation of molecules, thinner organic mats, and a greater degree of soil development (expression of A and Bw horizons) on the backslope under open cover than those under closed cover. In contrast, little to no effect of canopy was observed for soils at the footslope position, where the soil moisture content was highest and may have overshadowed the effects of canopy cover. Copyright 2023 The Regents of University of California, Davis campus. All Rights Reserved. Illustration by Rob Riedel.

be contributing to ground temperature dynamics across cover types at both slope positions.

The effect of organic mat thickness may be enhanced by topographically induced microclimates. North-facing soils near Caribou Peak have been shown to be cooler than south-facing soils in similar black spruce environments to our Fairbanks hillslope catena.[9] The cooler, north-facing soils were found to contain thick O horizons and weakly developed mineral soils.[9] In our study, the development of both A and Bw horizons in some profiles under open cover on the backslope and under closed cover on the low backslope coincided with overall increases in the oxidation of SOC compounds, whereas soil profiles without A horizons (soils under the open canopy on the low backslope and soils under the closed canopy on the backslope) showed lower SOC oxidation (Figures 4 and 9). Our findings indicate that microclimate conditions dictated by both canopy and slope position may result in warmer soils and increased freeze–thaw cycle frequency (Figure 3) as well as increased oxidation of SOC compounds, soil development, and decreased organic mat thickness on backslope and low backslope soils across a north-facing catena (Figure 9).

Previous work identified a buffering effect of the organic mat on the underlying soil temperature in permafrost environments, with a higher probability of permafrost in soils underlying thicker organic mats.[4,47,48] Canopy cover is known to regulate organic mat thickness in forested systems underlain with permafrost, with lower canopy cover percentages in larch forests previously found to result in thinner organic mats and warmer soil temperatures.[48] The larch forest experiment, conducted in northeastern Siberia, reported that understory mosses also played a role in buffering permafrost, compared with the thinner lichen mats,[48] likely due to insulating characteristics (low bulk density) of mosses and their ability to decrease soil temperatures via evapotranspiration.[48,49] The larch forest experiment also found thinner organic layers of 6.0 cm and higher ground temperatures (4.1°C to 4.4°C) in August under open canopy cover compared with 12.3 cm and 2.1°C to 2.9°C under closed cover.[48] Our work demonstrated that soils from the backslope position had lower organic mat thicknesses under open cover than under closed cover, potentially resulting in a compounded effect of open cover (reducing summer shade and increasing snow insulation) and thin organic mats (decreased ability to buffer against warm summer temperatures). In contrast, we observed the formation of thicker organic mats under open cover at both the low backslope and footslope positions. Therefore, the potential increase in the soil temperature from open canopy cover in downslope positions did not coincide with soil warming from thin organic mats.

We hypothesize that the thinner organic mats may have made soils under the open cover on the backslope position more vulnerable to air temperature penetration during warmer summer months, whereas snow cover insulated against cooler temperatures during the winter (Figure 9). This hypothesis is supported by (i) well-documented effect of tree canopy and organic mat thickness on soil temperature[4,47,48] (Figure 2), (ii) the higher oxidation state of carbon compounds under the open cover in the backslope soils (Figures 8 and 9), and (iii) the overall higher temperature values of subsurface soils measured under the open canopy compared with the closed canopy near the backslope position (Figure 2). Notably, although the role of organic mat thickness in mediating the soil temperature has been established,[4,47,48] the effect can depend on additional topographic factors including the steepness of the slope[50] and the slope aspect.[51] We would expect overall cooler temperatures and less direct sunlight to the entire hillslope due to the slope aspect—northwest facing—decreasing the effect of the canopy on summer soil temperatures.[51] A Northwest Territories boreal forest study examining the impact of spruce and paper birch canopy on active layer thickness in the discontinuous permafrost zone reported a modified effect of organic layer thickness on thaw depth depending on the degree of slope.[50] For example, more shallow slopes (6.99° and 3.45°) showed a stronger relationship between active layer depth and organic mat thickness versus steeper slopes (10.5°).[50] The authors suggested that the effect of organic mat thickness on active layer thickness (and thus soil temperature and permafrost thaw) may be decreased on steeper slopes due to slope transport processes and soil moisture. This aligns with our findings for soils on the backslope position, where organic mat thickness appeared to play a role in temperature-driven carbon chemistry differences in slopes of 5–7°. However, the footslope position (1–2°) did reflect the soil moisture and transport processes (resulting in carbon-rich soils and SOM composition unique to that slope position) that apparently diminished the effect of canopy cover. Future research should test the effect of organic mat thickness on soil temperature across hillslopes to identify how position-specific characteristics may modify that effect.

4.2 | Vegetation and soil moisture

The variable role of the canopy on SOM composition indicates that the impact of meter-scale differences in the cover type in thawing permafrost systems depends on multiple site factors (i.e., soil moisture, tree -type and associated canopy size, and the degree of SOM transport and accumulation[4,50,52]). For example, there may be circumstances that increase the vulnerability of permafrost soil to temperature-driven disturbance under open and closed cover, such as with the lower moisture and decreased organic mat thickness as we saw in the higher NOSC under open cover backslope soils from our experiment. The backslope-specific interaction of organic mat thickness and canopy cover is likely driving higher ground temperatures under the open cover, the subsequent impacts to carbon compound oxidation, and the difference in relative abundances of lignin-like and aliphatic compounds between open and closed cover.

We did see canopy-driven differences in the NOSC of specific compound classes at the lower slope positions, although we did see canopy-driven differences in the NOSC of the overall SOC at the backslope and low backslope positions. The lower NOSC of aliphatic and lignin-like compounds under open cover on the low backslope (compared with closed) and the higher NOSC in aliphatics and

aromatics under open cover on the footslope position are not easily explained by contrasting temperatures. Other factors, such as differences in vegetation type, could play a similar role in our study as in a Siberian canopy study that examined small-scale heterogeneity in the soil temperature and C flux across contrasting types of understory vegetation.[48] The Siberian larch canopy study found no canopy-driven differences in heterotrophic respiration, a finding that was attributed to the mediative effect of contrasting productivity in open (lichen) and closed (shrubs and mosses) vegetation species.[48] In our experiment, meter-scale differences in the distribution and type of vegetation biomass and productivity could explain the noted variation in NOSC under open and closed cover at the low backslope and backslope positions (Figure 1A,B). In addition, even if ground temperatures are not directly responsible for differences in SOM composition, contrasting soil temperatures can promote differences in biomass production, as observed in a snow manipulation study in an Arctic tundra experiment that tested the effect of soil warming on plant production.[53] The experiment found that, in addition to increased plant biomass reflecting the belowground influences of increased soil warming, subsurface soil moisture informed the canopy-driven impacts to ground temperature, as demonstrated by the role of soil moisture in canopy effect at the footslope position within our experiment.

The degree of SOC oxidation in active layer soils has been connected with both cryogenic history (i.e., cryoturbation, sorted circles, and patterned ground) and soil depth.[54] A carbon stock study in the Lena River Delta, Siberia, found an association between intensive cryogenesis (increased soil development driven by cryogenic processes such as sorting and patterned ground) and more oxidized SOC molecules. The same study found a notable association with depth; lower soil layers overlying permafrost in Cryosols presented more reduced conditions versus more SOC oxidation in surface soils.[54] We postulate that contrasting pedogenic processes, namely, cryogenesis, may have contributed to soil development in the backslope and low backslope positions in our study. For instance, we found less developed soil profiles containing shallow C material under closed cover at the backslope compared with more developed soil profiles including A and Bw horizons under closed cover on the low backslope, with more developed soils being found under thinner organic mats. The contrasting organic mat thickness may have allowed for greater cryogenesis in the soil profiles on the backslope (under open cover) and low backslope (under closed cover) that contained greater soil development and overall SOC oxidation. Further study of the combined influence of depth, organic mat thickness, and cryogenesis on SOC oxidation in hillslope soils may provide more information about carbon bioavailability as soils continue to experience increasing frequencies of freeze–thaw cycles.

4.3 | Hillslope processes

Soil properties and SOM composition exhibited differences across the toposequence regardless of the cover type where more acidic and wetter footslope soils contained greater percentages of carbon and nitrogen and a higher relative abundance of lignin-like compounds (Figure 7 and Table 2). Conversely, the drier, weakly developed backslope and low backslope soils contained less carbon and nitrogen in combination with a higher relative abundance of aliphatics. Erosional deposition and downslope redistribution of water-soluble SOC is likely one driver of the higher SOC content at the lower slope positions as the evidence for solifluction and soil creep was not observed at this site. The process of increased persistence of SOC materials in deposition landform positions compared with erosion positions is well known,[8,55,56] with a non-permafrost study finding accumulations of less transformed SOC at depositional positions as measured by the degree of decomposition (i.e., alkyl:O-alkyl ratio and aromaticity).[8] The erosion–deposition process of SOC accumulation at downslope positions is especially pertinent in permafrost environments where solifluction, organic matter accumulation, and cold temperatures provide ideal conditions for downslope movement and preservation of SOC.[10,57]

Soil wetness and elevation were identified as drivers of organic matter accumulation in permafrost environments in addition to impacts from climate.[10,22] Soil wetness was identified as both an indicator of water transport and water-holding capacity as well as an inhibitor of aerobic decomposition in permafrost-affected soils.[22] The accumulation of SOC content that we found in soils from the wetter footslope position aligns well with the peak richness observed in the same footslope soils than in soils from the drier backslope (Tables 2 and 3). The SOC molecular richness (referred to as peak richness), which demonstrates a wider variety of *m/z* peaks detected using FT-ICR-MS,[58] is supported by findings from an Arctic tundra hillslope experiment that reported a larger array of SOC molecules in downslope riparian soils than in upslope soils.[21] Our results confirm that the accumulation of SOC in the wetter downslope positions at the base of hillslopes is large,[10,22] with a wide variety of SOC molecules across all compound classes (Table 3).

The greater abundance of lignin-like compounds at the footslope position also aligns well with a prior work that identified accumulations of lignin in anaerobic soils due to the O_2 requirement of initial enzymes needed for the depolymerization of lignin molecules.[59,60] The presence of redox features was observed only in subsurface mineral horizons at the footslope position under both open and closed cover (Figure A1). The presence of redox features provides additional morphological evidence for poor drainage and O_2 limitations that would also coincide with the persistence of lignin molecules.[59,60] By contrast, the upslope positions were better drained and did not display the same lignin preservation, demonstrating an important topographic control on SOM composition. Other studies have confirmed the lack of O_2 requirements for the decomposition of simple carbon compounds such as aliphatics.[61] The higher oxidation of lignin-like compounds under open cover unique to the backslope position aligns well with our understanding of lignin degradation.[59,60]

Mineralogy has also been attributed to variations in SOC composition across hillslope positions via erosion and water transport.[8] The

higher mica percentages in our experiment at the footslope position may have offered more sorption sites to SOC molecules due to the permanent charge layer offered by phyllosilicates.[62] Greater sorption in footslope soils may have allowed for mineral protection from decomposition and oxidation, mitigating the impact of temperature in open versus closed cover. In contrast, soils at the backslope position had a higher quartz percentage, indicating the presence of soil minerals with fewer reactive sites (due to a lower charge density) for SOC protection and potentially allowing for soil temperature to play a larger role in SOC composition under open and closed cover. However, we recognize that the abundance of mica and quartz in the footslope positions compared with upslope positions may not be substantial enough to impact SOC composition (Figure A3), with soil moisture and erosional deposition playing a larger role in determining differences in carbon compound distribution and variety across the slope.

5 | CONCLUSIONS

Predictions of carbon decomposition and greenhouse gas emissions in boreal forests underlain by permafrost require an enhanced understanding of how small-scale differences (1–3 m) in canopy, organic mat thickness, mineralogy, and soil moisture may drive heterogeneity in soil temperature and carbon response at the meter scale. As local climate conditions continue to undergo changes in high-latitude environments, the upscaled impacts of canopy-driven ground temperature heterogeneity require additional investigation to more accurately predict how warming temperatures will impact permafrost thaw in high-latitude regions. Here, we tested the effect of both canopy cover and slope position on SOC abundance and composition. We found that differences in the composition and distribution of SOC under open and closed cover ranged from major to negligible depending on the topographic position (backslope and footslope soils, respectively) and that—overall—topography had a higher impact on SOC composition compared with open versus closed canopy within each topographic position. Differences in organic mat thickness, lower availability of mineral protection, and shifts in vegetation likely introduced meter-scale heterogeneity that contributed to the effect of the canopy on SOC composition observed at the backslope position. Notably, the higher moisture content and anaerobic conditions in soils at the footslope position may have decreased heterogeneity between open and closed cover positions, especially if anaerobic processes and metabolic pathways overshadowed the effect of cover type as predicted. Greater soil moisture contents in soils from the footslope position explain the similarities observed in SOC between open and closed cover. However, we observed SOC differences under open and closed cover at the low backslope position where moisture contents were comparable to backslope soils.

The increased SOC oxidation under open cover at the backslope position leads us to infer that moisture conditions and organic mat thickness influence soil temperature and SOC composition along the Y1 transect near Fairbanks, Alaska. As warming temperatures continue to destabilize permafrost landscapes, the role of the canopy in determining temperature-driven differences in SOC decomposition depends on the slope position. SOC composition at the carbon-rich footslope position did not reflect the same canopy-driven differences in oxidation and the relative abundance of SOC compounds as observed in upslope soils. We predict that canopy—in combination with organic mat thickness—on backslope positions may introduce variability in SOC decomposition dynamics and ultimately carbon loss. As temperatures continue to rise, accurate predictions for how that warming will impact forested permafrost landscapes require understanding the complex relationship between ground temperature, topography, and canopy cover.

ACKNOWLEDGMENTS

We would like to thank Mark Bowden, Tom Wietsma, Rosalie K. Chu, and Jason Toyoda for their expertise and assistance with this experiment. We would like to thank Adam Fund, Kristin McAdow, Gloria Ambrowiak, and the Soil Health Laboratory at Oregon State University for soil characterization analyses. We would like to thank Rob Riedel for his illustration work in this paper. This research was supported by the U.S. Department of Energy, Office of Science, Biological and Environmental Research as part of the Environmental System Science Program. The Pacific Northwest National Laboratory is operated for DOE by Battelle Memorial Institute under contract DE-AC05-76RL01830. A portion of this research was performed using EMSL (grid.436923.9), a DOE Office of Science user facility sponsored by the Department of Energy's Office of Biological and Environmental Research and located at the Pacific Northwest National Laboratory. EC Rooney's work on this project was partially funded by NSF Office of Polar Programs Award #2138937.

DATA AVAILABILITY STATEMENT

All the data and scripts are available at https://github.com/Erin-Rooney/Y1_fairbanks and are archived and searchable online at https://search.emsl.pnnl.gov (Project ID #50267).

ORCID

Erin C. Rooney https://orcid.org/0000-0002-9121-7699

REFERENCES

1. Biskaborn BK, Smith SL, Noetzli J, et al. Permafrost is warming at a global scale. *Nat Commun*. 2019;10(1):264. doi:10.1038/s41467-018-08240-4
2. Chasmer L, Quinton W, Hopkinson C, Petrone R, Whittington P. Vegetation canopy and radiation controls on permafrost plateau evolution within the discontinuous permafrost zone, Northwest Territories, Canada. *Permafr Periglac Process*. 2011;22(3):199-213. doi:10.1002/ppp.724
3. Chen L, Chen Z, Jia G, Zhou J, Zhao J, Zhang Z. Influences of forest cover on soil freeze-thaw dynamics and greenhouse gas emissions through the regulation of snow regimes: a comparison study of the farmland and forest plantation. *Sci Total Environ*. 2020;726:138403. doi:10.1016/j.scitotenv.2020.138403
4. Shur YL, Jorgenson MT. Patterns of permafrost formation and degradation in relation to climate and ecosystems. *Permafr Periglac Process*. 2007;18(1):7-19. doi:10.1002/ppp.582

5. Stuenzi SM, Boike J, Cable W, et al. Variability of the surface energy balance in permafrost-underlain boreal forest. *Biogeosciences*. 2021; 18(2):343-365. doi:10.5194/bg-18-343-2021
6. Williams TJ, Quinton WL. Modelling incoming radiation on a linear disturbance and its impact on the ground thermal regime in discontinuous permafrost. *Hydrol Process*. 2013;27(13):1854-1865. doi:10.1002/hyp.9792
7. Brooks JR, Flanagan LB, Ehleringer JR. Responses of boreal conifers to climate fluctuations: indications from tree-ring widths and carbon isotope analyses. *Can J For Res*. 1998;28(4):524-533. doi:10.1139/cjfr-28-4-524
8. Berhe AA, Harden JW, Torn MS, Kleber M, Burton SD, Harte J. Persistence of soil organic matter in eroding versus depositional landform positions. *J Geophys Res Biogeo*. 2012;117(G2):G02019. doi:10.1029/2011JG001790
9. Ping CL, Michaelson GJ, Packee EC, Stiles CA, Swanson DK, Yoshikawa K. Soil catena sequences and fire ecology in the boreal Forest of Alaska. *Soil Sci Soc Am J*. 2005;69(6):1761-1772. doi:10.2136/sssaj2004.0139
10. Shelef E, Rowland JC, Wilson CJ, et al. Large uncertainty in permafrost carbon stocks due to hillslope soil deposits. *Geophys Res Lett*. 2017;44(12):6134-6144. doi:10.1002/2017GL073823
11. Quinton WL, Hayashi M, Chasmer LE. Peatland hydrology of discontinuous permafrost in the Northwest Territories: overview and synthesis. *Can Water Res J*. 2009;34(4):311-328. doi:10.4296/cwrj3404311
12. Joss H, Patzner M, Maisch M, Mueller CW, Kappler A, Bryce C. Cryoturbation impacts iron-organic carbon associations along a permafrost soil chronosequence in northern Alaska. *Geoderma*. 2022;413: 115738. doi:10.1016/j.geoderma.2022.115738
13. Xu C, Guo L, Ping C-L, White DM. Chemical and isotopic characterization of size-fractionated organic matter from cryoturbated tundra soils, northern Alaska. *J Geophys Res*. 2009;114:G03002. doi:10.1029/2008JG000846
14. Brooks PD, Grogan P, Templer PH, Groffman P, Öquist MG, Schimel J. Carbon and nitrogen cycling in snow-covered environments. *Geogr Compass*. 2011;5(9):682-699. doi:10.1111/j.1749-8198.2011.00420.x
15. Schmidt SK, Lipson DA. Microbial growth under the snow: implications for nutrient and allelochemical availability in temperate soils. *Plant and Soil*. 2004;259(1/2):1-7. doi:10.1023/B:PLSO.0000020933.32473.7e
16. Bailey VL, Pries CH, Lajtha K. What do we know about soil carbon destabilization? *Environ Res Lett*. 2019;14(8):083004. doi:10.1088/1748-9326/ab2c11
17. Edwards LM. The effects of soil freeze–thaw on soil aggregate breakdown and concomitant sediment flow in Prince Edward Island: a review. *Can J Soil Sci*. 2013;93(4):459-472. doi:10.4141/cjss2012-059
18. Makusa GP, Bradshaw SL, Berns E, Benson CH, Knutsson S. Freeze–thaw cycling concurrent with cation exchange and the hydraulic conductivity of geosynthetic clay liners. *Can Geotech J*. 2014;51(6):591-598. doi:10.1139/cgj-2013-0127
19. Yu X, Zhang Y, Zhao H, Lu X, Wang G. Freeze-thaw effects on sorption/desorption of dissolved organic carbon in wetland soils. *Chin Geogr Sci*. 2010;20(3):209-217. doi:10.1007/s11769-010-0209-7
20. Ping CL, Jastrow JD, Jorgenson MT, Michaelson GJ, Shur YL. Permafrost soils and carbon cycling. *Soil*. 2015;1:147-171. doi:10.5194/soil-1-147-2015
21. Lynch LM, Machmuller MB, Boot CM, et al. Dissolved organic matter chemistry and transport along an Arctic tundra hillslope. *Global Biogeochem Cycles*. 2019;33(1):47-62. doi:10.1029/2018GB006030
22. Mishra U, Hugelius G, Shelef E, et al. Spatial heterogeneity and environmental predictors of permafrost region soil organic carbon stocks. *Sci Adv*. 2021;7(9):eaaz5236. doi:10.1126/sciadv.aaz5236
23. Harden JW, Koven CD, Ping C-L, et al. Field information links permafrost carbon to physical vulnerabilities of thawing. *Geophys Res Lett*. 2012;39(15):L15704. doi:10.1029/2012GL051958
24. Schuur EAG, McGuire AD, Schädel C, et al. Climate change and the permafrost carbon feedback. *Nature*. 2015;520(7546):171-179. doi:10.1038/nature14338
25. Tarnocai C, Canadell JG, Schuur EAG, Kuhry P, Mazhitova G, Zimov S. Soil organic carbon pools in the northern circumpolar permafrost region. *Global Biogeochem Cycles*. 2009;23(2):n/a-n/a. doi:10.1029/2008GB003327
26. USGS, S. of A., Polar Geospatial Center, U. of M., National Science Foundation, National Geospatial-Intelligence Agency & DigitalGlobe. Arctic DEM. 2018.
27. Wang B, Hults CP, Eberl DD, Woodruff LG, Cannon WF, Gough LP. Studies by the U.S. Geological Survey in Alaska, volume 15: soil mineralogy and geochemistry along a north-south transect in Alaska and the relation to source-rock terrane. Reston, Virginia. 2019.
28. Brown J, Kreig RA. *Guidebook to permafrost and related features along the Elliott and Dalton highways, fox to Prudhoe Bay, Alaska*. Alaska Division of Geological & Geophysical Surveys; 1983. doi:10.14509/266
29. Péwé TL. An observation of wind-blown silt. *J Geol*. 1951;59(4):399-401. doi:10.1086/625877
30. Soil Survey Staff. *Keys to Soil Taxonomy*. 12th ed. USDA-Natural Resources Conservation Service; 2014.
31. Soil Survey Staff, Natural Resources Conservation Service, United States Department of Agriculture. Soil Series Classification Database, 2022. Available online at https://soilseries.sc.egov.usda.gov. Accessed November, 2022.
32. Gee GW, Bauder JW. Particle-size analysis. In: Klute A, ed. *Methods of Soil Analysis. Part 1*. Agron. Monogr. 9. ASA and SSSA; 1986: 383-411.
33. Agriculture, F. and C.D. Nature conservation practice note: measurement of diameter at breast height (DBH). 2006.
34. D'Eon SP, Magasi LP, Lachance D, DesRochers P. Canada's national forest health monitoring plot network. Manual on plot establishment and monitoring. Chalk River, Ontario. 1994.
35. Kibele J, Clark J. State of Alaska's Salmon and People Regional Boundaries. 2018. 10.5063/F1125QWP
36. Rooney EC, Bailey VL, Patel KF, et al. Soil pore network response to freeze-thaw cycles in permafrostaggregates. *Geoderma*. 2022;411: 115674. doi:10.1016/j.geoderma.2021.115674
37. Boswell EP, Thompson AM, Balster NJ, Bajcz AW. Novel determination of effective freeze–thaw cycles as drivers of ecosystem change. *J Environ Qual*. 2020;49(2):314-323. doi:10.1002/jeq2.20053
38. Patel KF. fticrrr. R Package Version v0.1.0. 2020. doi:10.5281/zenodo.3893246
39. Graham EB, Tfaily MM, Crump AR, et al. Carbon inputs from riparian vegetation limit oxidation of physically bound organic carbon via biochemical and thermodynamic processes. *J Geophys Res Biogeo*. 2017; 122(12):3188-3205. doi:10.1002/2017JG003967
40. LaRowe DE, van Cappellen P. Degradation of natural organic matter: a thermodynamic analysis. *Geochim Cosmochim Acta*. 2011;75(8): 2030-2042. doi:10.1016/j.gca.2011.01.020
41. R Core Team. R: A language and environment for statistical computing. 2020.
42. Wickham H, François R, Henry L. Dplyr: a grammar of data manipulation. 2020.
43. Oksanen J, Blanchet FG, Kindt R. Vegan: community ecology package. 2019.
44. Wickham H. *ggplot2: Elegant Graphics for Data Analysis*. Springer; 2016.
45. Kahle D, Wickham H. Ggmap: spatial visualization with ggplot2. *The R Journal*. 2013;5(1):144-161. https://journal.r-project.org/archive/2013-1/kahle-wickham.pdf

46. IUSS Working Group WRB. *World Reference Base for soil resources 2014, update 2015 international soil classification system for naming soils and creating legends for soil maps*World Soil Resources Reports No. 106. FAO; 2015.
47. Johnson KD, Harden JW, David McGuire A, Clark M, Yuan F, Finley AO. Permafrost and organic layer interactions over a climate gradient in a discontinuous permafrost zone. *Environ Res Lett*. 2013; 8(3):035028. doi:10.1088/1748-9326/8/3/035028
48. Loranty MM, Berner LT, Taber ED, et al. Understory vegetation mediates permafrost active layer dynamics and carbon dioxide fluxes in open-canopy larch forests of northeastern Siberia. *PLoS ONE*. 2018; 13(3):e0194014. doi:10.1371/journal.pone.0194014
49. Romanovsky VE, Osterkamp TE. Effects of unfrozen water on heat and mass transport processes in the active layer and permafrost. *Permafr Periglac Process*. 2000;11(3):219-239. doi:10.1002/1099-1530(200007/09)11:33.0.CO;2-7
50. Fisher JP, Estop-Aragonés C, Thierry A, et al. The influence of vegetation and soil characteristics on active-layer thickness of permafrost soils in boreal forest. *Glob Chang Biol*. 2016;22(9):3127-3140. doi:10.1111/gcb.13248
51. Måren IE, Karki S, Prajapati C, Yadav RK, Shrestha BB. Facing north or south: does slope aspect impact forest stand characteristics and soil properties in a semiarid trans-Himalayan valley? *J Arid Environ*. 2015;121:112-123. doi:10.1016/j.jaridenv.2015.06.004
52. Kropp H, Loranty MM, Natali SM, et al. Tree density influences ecohydrological drivers of plant–water relations in a larch boreal forest in Siberia. *Ecohydrology*. 2019;12(7):e2132. doi:10.1002/eco.2132
53. Natali SM, Schuur EAG, Rubin RL. Increased plant productivity in Alaskan tundra as a result of experimental warming of soil and permafrost. *J Ecol*. 2012;100(2):488-498. doi:10.1111/j.1365-2745.2011.01925.x
54. Polyakov V, Orlova K, Abakumov E. Evaluation of carbon stocks in the soils of Lena River Delta on the basis of application of "dry combustion" and Tyurin's methods of carbon determination. *BioComm*. 2017;62:67-72. doi:10.21638/11701/spbu03.2017.202
55. Berhe AA, Harte J, Harden JW, Torn MS. The significance of the erosion-induced terrestrial carbon sink. *Bioscience*. 2007;57(4):337-346. doi:10.1641/B570408
56. Stallard RF. Terrestrial sedimentation and the carbon cycle: coupling weathering and erosion to carbon burial. *Global Biogeochem Cycles*. 1998;12(2):231-257. doi:10.1029/98GB00741
57. Ramage JL, Fortier D, Hugelius G, Lantuit H, Morgenstern A. Distribution of carbon and nitrogen along hillslopes in three valleys on Herschel Island, Yukon territory, Canada. *Catena*. 2019;178:132-140. doi:10.1016/j.catena.2019.02.029
58. Smith AP, Bond-Lamberty B, Benscoter BW, et al. Shifts in pore connectivity from precipitation versus groundwater rewetting increases soil carbon loss after drought. *Nat Commun*. 2017;8(1):1335. doi:10.1038/s41467-017-01320-x
59. Freeman C, Ostle N, Kang H. An enzymic "latch" on a global carbon store. *Nature*. 2001;409(6817):149. doi:10.1038/35051650
60. Huang W, Ye C, Hockaday WC, Hall SJ. Trade-offs in soil carbon protection mechanisms under aerobic and anaerobic conditions. *Glob Chang Biol*. 2020;26(6):3726-3737. doi:10.1111/gcb.15100
61. Kirk TK, Farrell RL. Enzymatic "combustion": the microbial degradation of lignin. *Annu Rev Microbiol*. 1987;41(1):465-501. doi:10.1146/annurev.mi.41.100187.002341
62. Kögel-Knabner I, Guggenberger G, Kleber M, et al. Organo-mineral associations in temperate soils: integrating biology, mineralogy, and organic matter chemistry. *J Plant Nutr Soil Sci*. 2008;171(1):61-82. doi:10.1002/jpln.200700048
63. Seidel M, Beck M, Riedel T, et al. Biogeochemistry of dissolved organic matter in an anoxic intertidal creek bank. *Geochim Cosmochim Acta*. 2014;140:418-434. doi:10.1016/j.gca.2014.05.038

How to cite this article: Rooney EC, Bailey VL, Patel KF, Kholodov A, Golightly H, Lybrand RA. Topography and canopy cover influence soil organic carbon composition and distribution across a forested hillslope in the discontinuous permafrost zone. *Permafrost and Periglac Process*. 2023;34(3): 331-358. doi:10.1002/ppp.2200

APPENDIX A

Topography and canopy cover influence soil organic carbon composition and distribution across a forested hillslope in the discontinuous permafrost zone.

A.1 | Extensive overview of the Fourier-transform ion cyclotron resonance mass spectrometry (measurement, analysis, and data visualization approach

Compound classification was conducted via modified aromaticity index (AImod) (Equation 1), hydrogen-to-carbon (H/C) and oxygen-to-carbon (O/C) ratios, and the nominal oxidation state of carbon (NOSC) (Equation 2).[40]

Equation 1. Aromaticity index (AImod)

$$\mathrm{AImod} = \frac{1 + \mathrm{C} - (0.5 \times \mathrm{O}) - \mathrm{S} - (0.5 \times (\mathrm{N} + \mathrm{P} + \mathrm{H}))}{(\mathrm{C} - (0.5 \times \mathrm{O}) - \mathrm{S} - \mathrm{N} - \mathrm{P}}$$

Equation 2. NOSC

$$\mathrm{NOSC} = \frac{4 - (((4 \times \mathrm{C}) + \mathrm{H} - (3 \times \mathrm{N}) - (2 \times \mathrm{O}) - (2 \times \mathrm{S}))}{\mathrm{C}}$$

in which C = carbon, H = hydrogen, O = oxygen, S = sulfur, N = nitrogen, and P = phosphorus.

Identified molecules were separated into four compound classes using the AImod and H/C and O/C ratios. Following Seidel et al. (2014),[63] we used formulas, rather than molecular structure, to delineate biomolecular groupings. The Seidel classification system (organized by molecular O/C and H/C ratios) defines compound classes as (i) condensed aromatics (AImod > 0.66), (ii) aromatic compounds (0.66 > AImod > 0.50), (iii) highly unsaturated and lignin-like compounds (AImod < 0.50 and H/C < 1.5), and (iv) aliphatic compounds (> H/C ≥ 1.5) (Seidel et al. 2014[63]). Relative abundances were calculated as the number of unique peaks (formulas) within a specific compound class compared with the total number of unique peaks across all compound classes.

A.2 | Extensive overview of the X-ray diffraction measurement and analysis

Minerals were quantified by the Rietveld method using TOPAS (v6, Bruker AXS). The Rietveld method combines calculated X-ray diffraction patterns from the substituent minerals to provide the best fit with the observed pattern. For each mineral, the scale factor, cell parameters (constrained within ~0.5% of the expected values), and crystallite size (constrained between 50 and 500 nm) were refined. A preferred orientation correction was refined for minerals consisting of platy morphologies. The scale factors from the Rietveld refinement were used to determine the relative quantities of the minerals, which are scaled to a total of 100%. Allowing for the minimization of structural factors including lattice parameters, intensity, coherent scattering domain size, and preferred orientation bias, final model results were achieved with typical weighted profile residual (R_{wp}) ranging from 5.43% to 12 %.

TABLE A1 Particle size class as determined by hydrometer method

		Closed cover (%)	Open cover (%)
Backslope	Clay	17 ± 2	17 ± 1
	Silt	45 ± 3	56 ± 6
	Sand	38 ± 3	27 ± 7
	Textural class	Loam	Silt loam
Low backslope	Clay	21 ± 2	19 ± 1
	Silt	51 ± 4	60 ± 3
	Sand	28 ± 5	21 ± 3
	Textural class	Silt loam	Silt loam
Footslope	Clay	20 ± 1	18 ± 1
	Silt	72 ± 2	72 ± 4
	Sand	8 ± 2	11 ± 4
	Textural class	Silt loam	Silt loam

Note. All values are reported in percentages with standard error. Sand is defined as 50 μm to 2 mm, silt is defined as 2 to 50 μm, and clay is defined as <2 μm.

TABLE A2 Significant effects of slope position, cover type, and their interaction on soil properties

	Slope position	Cover type	Interaction
Gravimetric water (%)	0.0004	–	–
TC (%)	<0.0001	–	–
TN (%)	<0.0001	–	–
C:N ratio	0.0006	–	0.002
SOM (%)	–	–	–
Organic mat thickness	0.0006	–	0.008
pH	<0.0001	–	–

Note. *p* values are presented (ANOVAs only).
Abbreviations: SOM, soil organic matter; TC, total nitrogen; TN, total nitrogen.

TABLE A3 Mineralogy abundances as determined by X-ray diffraction

	Mineral	Backslope (%)	Low backslope (%)	Footslope (%)
Closed	Albite	15.1 ± 0.8	16 ± 0.7	13.4 ± 0.3
	Ankerite	0.8 ± 0.3	0.8 ± 0.1	0.3 ± 0.1
	Anorthite	14.8 ± 0.4	16.7 ± 1	14.4 ± 0.3
	Chlorite	5.9 ± 0.8	5.3 ± 0.4	7.6 ± 0.3
	Hornblende	4.1 ± 0.1	4.3 ± 0.4	3.9 ± 0.1
	Mica	9.7 ± 0.7	9.3 ± 0.7	14.6 ± 0.8
	Microcline	3.5 ± 0.9	4 ± 0.8	5.8 ± 0.4
	Quartz	46 ± 1.8	43.5 ± 0.9	40 ± 0.6
Open	Albite	15.3 ± 0.6	14.7 ± 0.3	14 ± 0.5
	Ankerite	0.6 ± 0.1	0.5 ± 0.1	0.3 ± 0.1
	Anorthite	16.7 ± 1.1	16.6 ± 0.7	15.1 ± 0.6
	Chlorite	5.6 ± 0.5	6.2 ± 0.3	6.7 ± 0.6
	Hornblende	4.6 ± 0.6	4.7 ± 0.2	3.7 ± 0.4
	Mica	9.7 ± 0.6	10.1 ± 0.3	14 ± 1
	Microcline	4.8 ± 1.4	4.9 ± 0.9	4.9 ± 0.8
	Quartz	42.7 ± 1.8	42.1 ± 0.7	41.3 ± 1.4

Note. All values are in percentages with standard error.

TABLE A4 TC and TN by horizon for the backslope position

Backslope	Replicate	Horizon	Depth (cm)	TC (%)	TN (%)
Closed	C–A	Bg1	26–49	0.49 ± 0.02	0.03 ± 0
	C–B	Bg1	28–50	1.43 ± 0.01	0.08 ± 0
	C–C	Bg1	22–44	1.1 ± 0.01	0.05 ± 0
			Grand mean	1.01 ± 0.14	0.05 ± 0.01
Open	O–A	Bg1	19–46	0.78 ± 0	0.05 ± 0
	O–B	Bg2	36–48	0.28 ± 0	0.02 ± 0
	O–B	Bg3	48–53	0.41 ± 0	0.03 ± 0
	O–B	Bg4	53–57	0.48 ± 0	0.03 ± 0
	O–C	Bg2	19–42	0.24 ± 0.01	0.01 ± 0
			Grand mean	0.44 ± 0.05	0.03 ± 0

Note. All values are in percentages with standard error for instrument/analytical replicates. No statistical differences are found between open and closed cover.
Abbreviations: TC, total carbon; TN, total nitrogen.

TABLE A5 TC and TN by horizon for the low backslope position

Low backslope	Replicate	Horizon	Depth (cm)	TC (%)	TN (%)
Closed	C–A	A	26–35	3.96 ± 0.01	0.25 ± 0
	C–A	Bg1	35–40	0.57 ± 0	0.03 ± 0
	C–A	Bg2	40–45	0.41 ± 0	0.03 ± 0
	C–B	Bg	19–44	1.17 ± 0.01	0.06 ± 0
	C–C	Bg2	38–41	1.25 ± 0.01	0.07 ± 0
			Grand mean	1.43 ± 0.29	0.08 ± 0.02
Open	O–A	Bg1	23–35	1.31 ± 0	0.09 ± 0
	O–A	Bg2	35–39	0.57 ± 0	0.03 ± 0
	O–A	Bg3	39–42	0.46 ± 0	0.03 ± 0
	O–B	Bg1	29–40	5.63 ± 0	0.28 ± 0
	O–B	Bg2	40–44	1.48 ± 0	0.09 ± 0
	O–B	Bg3	44–48	1.31 ± 0	0.07 ± 0
	O–C	Bg1	30–43	2.26 ± 0.01	0.12 ± 0
	O–C	Bg2	43–48	1.52 ± 0	0.07 ± 0
			Grand mean	1.82 ± 0.32	0.1 ± 0.02

Note. No statistical differences are found between open and closed cover. All values are in percentages.
Abbreviations: TC, total carbon; TN, total nitrogen.

TABLE A6 TC and TN by horizon for the footslope position

Footslope	Replicate	Horizon	Depth (cm)	TC (%)	TN (%)
Closed	C–A	Bg2	38–43	1.28 ± 0.08	0.08 ± 0
	C–A	Bg3	43–48	1.75 ± 0	0.11 ± 0
	C–B	Bg1	25–39	1.55 ± 0	0.09 ± 0
	C–B	Bg2	39–43	1.32 ± 0	0.08 ± 0
	C–B	Bg3	43–48	1.42 ± 0	0.08 ± 0
	C–C	Bg1	29–35	4.05 ± 0.01	0.21 ± 0
	C–C	Bg2	35–40	6.69 ± 0.01	0.31 ± 0
	C–C	Bg3	40–45	3.49 ± 0	0.16 ± 0
			Grand mean	2.54 ± 0.35	0.13 ± 0.02
Open	O–A	Bg1	42–48	1.61 ± 0.01	0.09 ± 0
	O–A	Bg2	49–54	1.49 ± 0	0.09 ± 0
	O–B	Bg1	33–35	6.25 ± 0.01	0.28 ± 0.01
	O–B	Bg2	35–39	5.41 ± 0.01	0.3 ± 0
	O–B	Oe	39–44	15.7 ± 0.02	0.68 ± 0
	O–C	Bg1	33–45	1.19 ± 0.01	0.07 ± 0
	O–C	Bg2	45–50	2.28 ± 0	0.1 ± 0
	O–C	Bg3	50–54	1.5 ± 0.01	0.08 ± 0
			Grand mean	4.43 ± 0.97	0.21 ± 0.04

Note. No statistical differences are found between open and closed cover. All values are in percentages.
Abbreviations: TC, total carbon; TN, total nitrogen.

TABLE A7 Relative abundances of carbon compound classes with comparisons between slope positions

	Class	Backslope	Low backslope	Footslope
Closed	Aliphatic	38.79 ± 2.56 a	31.07 ± 1.64 ab	29.64 ± 0.95 b
	Unsaturated/lignin	52.85 ± 2.32 a	57.17 ± 2.05 a	60.15 ± 0.64 a
	Aromatic	3.44 ± 1.48 a	7.17 ± 0.45 a	6.92 ± 0.58 a
	Condensed aromatic	4.92 ± 1.28 a	4.6 ± 0.25 a	3.29 ± 0.24 a
Open	Aliphatic	35.08 ± 3.05 a	34.58 ± 4.1 a	27.95 ± 1.95 a
	Unsaturated/lignin	52.62 ± 1.69 b	57.56 ± 3.44 ab	64.31 ± 0.78 a
	Aromatic	2.2 ± 0.83 a	4.03 ± 0.69 a	4.41 ± 1.38 a
	Condensed aromatic	10.1 ± 0.75 a	3.84 ± 0.14 b	3.33 ± 0.24 b

Note. Differences were determined at significance 0.05 via ANOVA and Tukey HSD tests. Statistical comparisons are made between slope positions within cover types. Letters denote differences between slope positions within each compound class and cover type as determined by Tukey HSD tests ($P < 0.05$). All values are in percentages (%).

TABLE A8 Relative abundances of carbon compound classes with comparisons between cover types at each slope position

	Backslope		Low backslope		Footslope	
Class	Closed	Open	Closed	Open	Closed	Open
Aliphatic	38.79 ± 2.56	35.08 ± 3.05	31.07 ± 1.64	34.58 ± 4.1	29.64 ± 0.95	27.95 ± 1.95
Lignin-like	52.85 ± 2.32	52.62 ± 1.69	57.17 ± 2.05	57.56 ± 3.44	60.15 ± 0.64	64.31 ± 0.78*
Aromatic	3.44 ± 1.48	2.2 ± 0.83	7.17 ± 0.45	4.03 ± 0.69*	6.92 ± 0.58	4.41 ± 1.38
Condensed aromatic	4.92 ± 1.28	10.1 ± 0.75*	4.6 ± 0.25	3.84 ± 0.14	3.29 ± 0.24	3.33 ± 0.24

Note. Differences were determined at significance 0.05 via ANOVA test. Statistical comparisons are made between cover types within each slope position with statistical significance noted by asterisks. All values are in percentages (%).

TABLE A9 Relative abundances of carbon compound classes by horizon for all plots at the backslope position

Backslope	Replicate	Horizon	Depth (cm)	Aliphatic	Unsaturated/lignin	Aromatic	Condensed aromatic
Closed	C–A	Bg1	26–49	43.81	48.27	1.73	6.19
	C–B	Bg1	28–50	35.44	55.83	6.38	2.36
	C–C	Bg1	22–44	37.11	54.44	2.22	6.22
			Grand mean	38.79 ± 2.56	52.85 ± 2.32	3.44 ± 1.48	4.92 ± 1.28
Open	O–A	Bg1	19–46	29.2	55.41	3.85	11.54
	O–B	Bg2	36–48	42.76	49.82	1.06	6.36
	O–B	Bg3	48–53	33.73	53.37	1.79	11.11
	O–B	Bg4	53–57	35.98	54.18	1.46	8.37
	O–C	Oi	0–8	37.89	50	1.55	10.57
			Grand mean	35.08 ± 3.05	52.62 ± 1.69	2.2 ± 0.83	10.1 ± 0.75

Note. Statistical comparisons are made between grand means of open versus closed cover soils. All values are in percentages (%).

TABLE A10 Relative abundances of carbon compound classes by horizon for all plots at the low backslope position

Low backslope	Replicate	Horizon	Depth (cm)	Aliphatic	Unsaturated/lignin	Aromatic	Condensed aromatic
Closed	C–A	A	26–35	24.87	60.51	9.32	5.3
	C–A	Bg1	35–40	34.36	56.78	3.76	5.1
	C–A	Bg2	40–45	34.27	57.76	4.06	3.92
	C–B	Bg	19–44	34.27	53.1	7.82	4.82
	C–C	Bg1	21–38	32.84	56.63	7.65	2.88
	C–C	Bg2	38–41	26.48	61.01	7.66	4.85
	C–C	Bg3	41–45	26.07	62.36	6.63	4.94
			Grand mean	31.07 ± 1.64	57.17 ± 2.05	7.17 ± 0.45	4.6 ± 0.25
Open	O–A	Bg1	23–35	42.31	52.94	2.09	2.66
	O–A	Bg2	35–39	41.67	51.11	3.47	3.75
	O–A	Bg3	39–42	44.55	48	2.36	5.09
	O–B	Bg1	29–40	30.12	60.34	6.09	3.46
	O–B	Bg2	40–44	28.81	63.69	4.08	3.42
	O–B	Bg3	44–48	30.58	60.5	5.01	3.92
	O–C	Bg1	30–43	32.77	59.11	3.93	4.19
	O–C	Bg2	43–48	29.78	61.67	4.56	4
			Grand mean	34.58 ± 4.1	57.56 ± 3.44	4.03 ± 0.69	3.84 ± 0.14

Note. All values are in percentages (%).

TABLE A11 Relative abundances of carbon compound classes by horizon for all plots at the footslope position

Footslope	Replicate	Horizon	Depth, cm	Aliphatic	Unsaturated/lignin	Aromatic	Condensed aromatic
Closed	C–A	Bg1	29–38	33.87	56.96	6.88	2.29
	C–A	Bg2	38–43	29.61	62.11	5.14	3.14
	C–A	Bg3	43–48	30.09	61.27	5.06	3.57
	C–B	Bg1	25–39	25.9	64.13	6.89	3.08
	C–B	Bg2	39–43	31.59	56.16	8.14	4.11
	C–B	Bg3	43–48	29.51	58.51	8.04	3.93
	C–C	Bg1	29–35	30.46	59.91	7.07	2.56
	C–C	Bg2	35–40	27.54	62.55	6.78	3.13
	C–C	Bg3	40–45	26.58	61.87	7.75	3.8
			Grand mean	29.64 ± 0.95	60.15 ± 0.64	6.92 ± 0.58	3.29 ± 0.24
Open	O–A	Bg1	42–48	29.07	64.84	3.25	2.85
	O–A	Bg2	49–54	31.85	61.17	2.54	4.44
	O–B	Oe/Bg	33–35	24.44	64.89	7.17	3.5
	O–B	Bg1	35–39	23.47	66.64	6.92	2.97
	O–B	Bg2	39–44	24.55	64.55	7.39	3.51
	O–C	Bg1	33–45	26.14	65.91	4.26	3.69
	O–C	Bg2	45–50	31.51	64.11	2.3	2.08
	O–C	Bg3	50–54	28.9	64.57	3.38	3.15
			Grand mean	27.95 ± 1.95	64.31 ± 0.78	4.41 ± 1.38	3.33 ± 0.24

Note. All values are in percentages (%).

FIGURE A1 Photograph of a soil sample from the closed footslope position containing Oi, Oa, and Bg horizons. The white arrows are pointing to oxidized iron concentrations observed within the Bg horizon. Oxidized iron concentrations are observed in the footslope soils under both open and closed cover

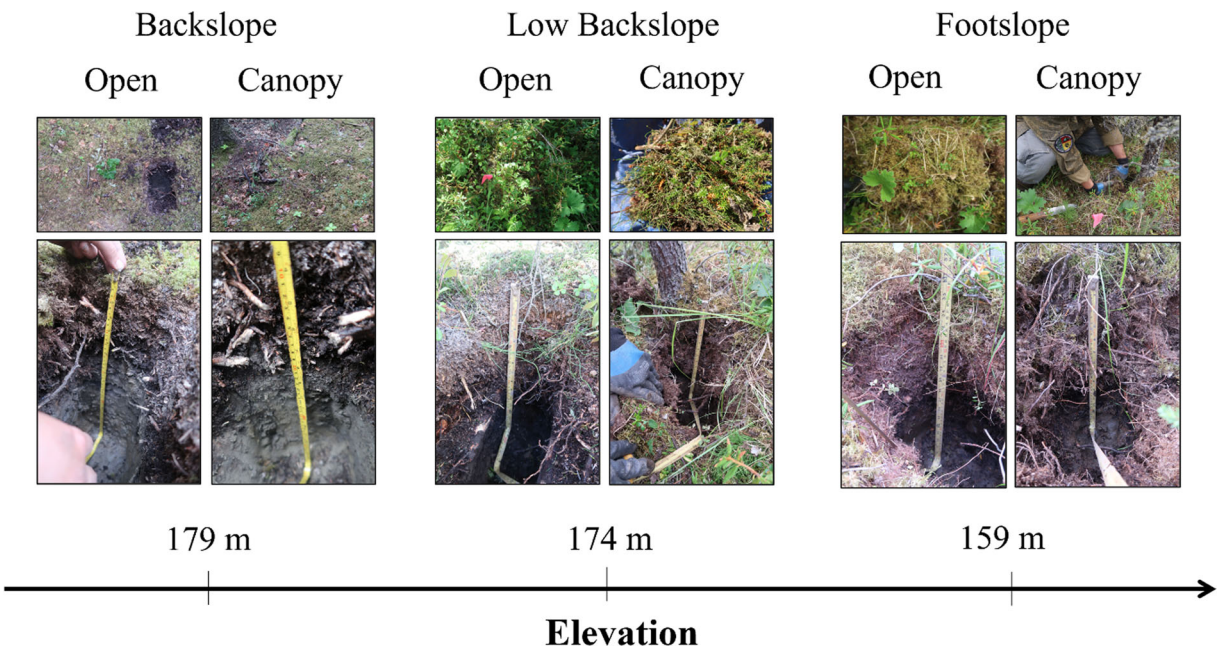

FIGURE A2 General site, vegetation, and soil profile photographs from backslope, low backslope, and footslope positions under both open and closed cover across the hillslope gradient. Three pits per slope position × cover type combination are sampled. We present one photo from each slope position × cover type in this figure as a demonstrative example. The supporting soil morphological data for each profile are provided in Figure 4

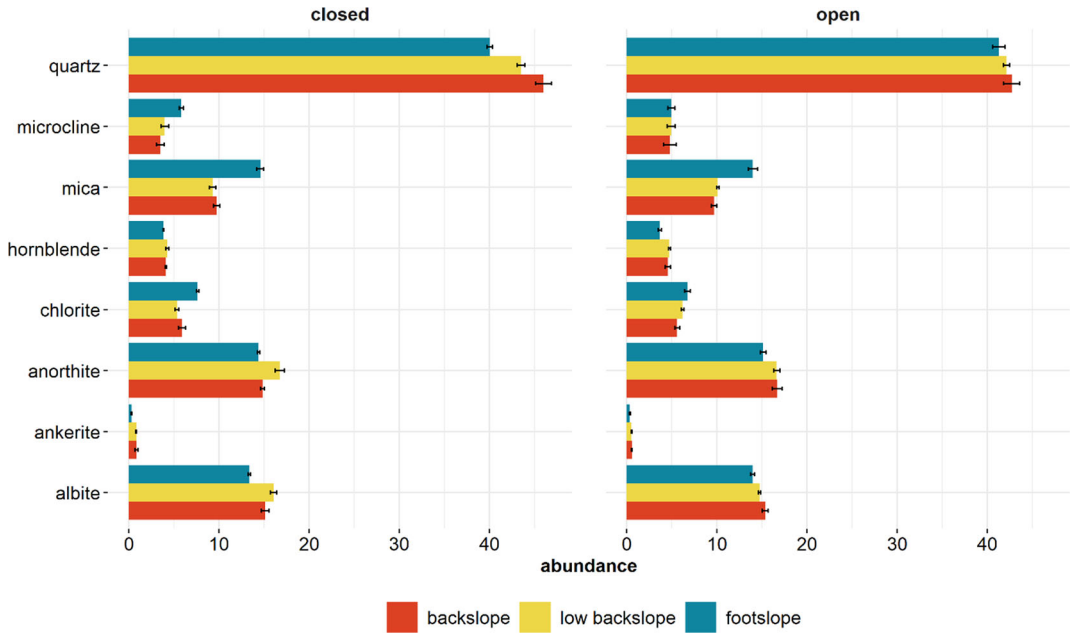

FIGURE A3 Mineral composition and abundances with comparisons between hillslope positions and cover types as identified using X-ray diffraction. Statistical comparisons are made within cover types between slope positions (backslope, low backslope, and footslope) and are summarized in Table A1 and Figures A2–A4. All values are in percentages (%)

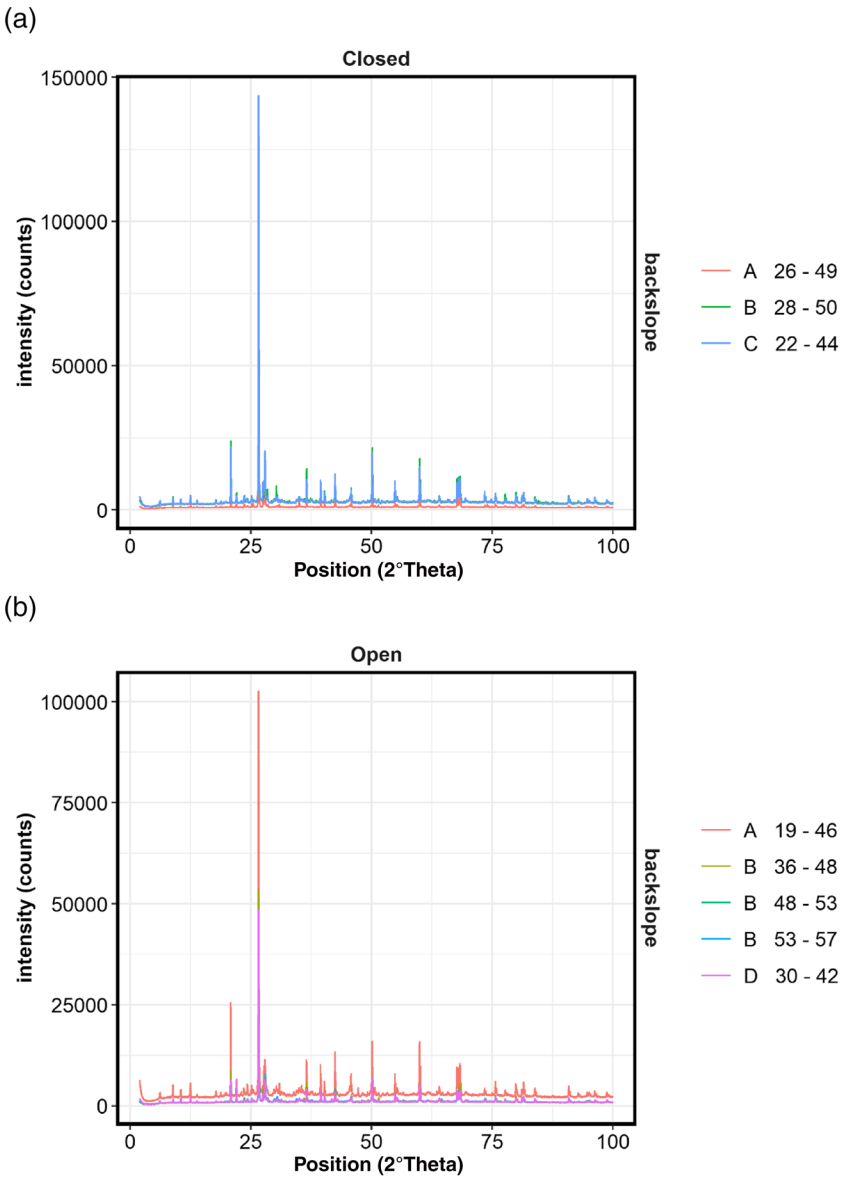

FIGURE A4 Diffractogram patterns from the X-ray diffraction analysis of the mineral soils at the backslope position under (A) closed and (B) open cover

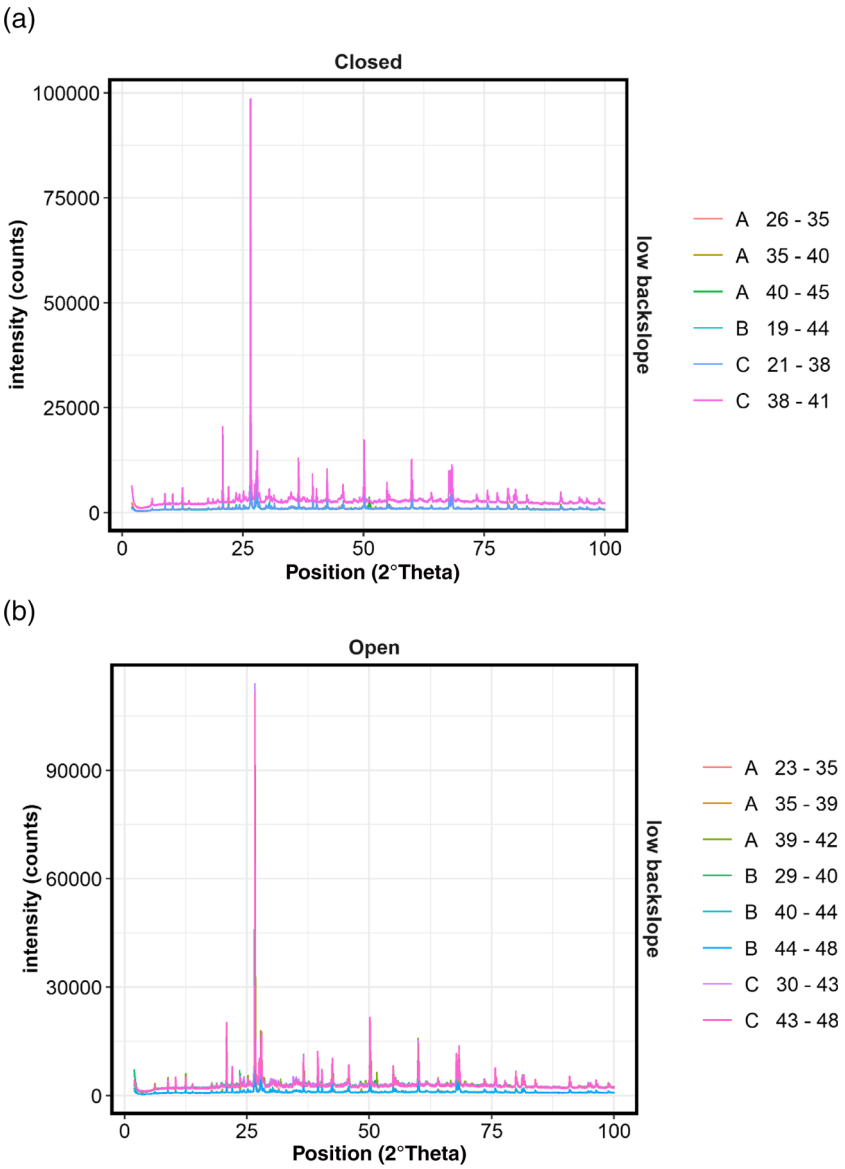

FIGURE A5 Diffractogram patterns from the X-ray diffraction analysis of the mineral soils at the low backslope position under (A) closed and (B) open cover

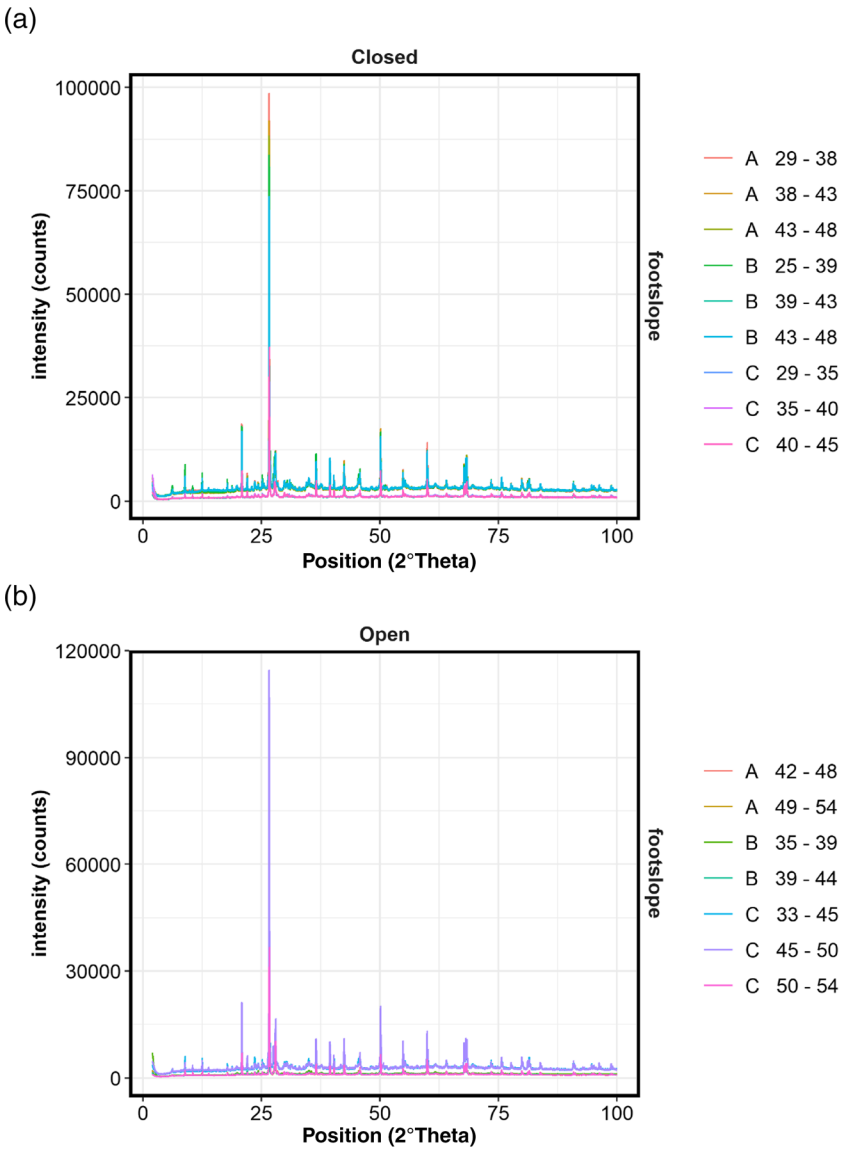

FIGURE A6 Diffractogram patterns from the X-ray diffraction analysis of the mineral soils at the footslope position under (A) closed and (B) open cover

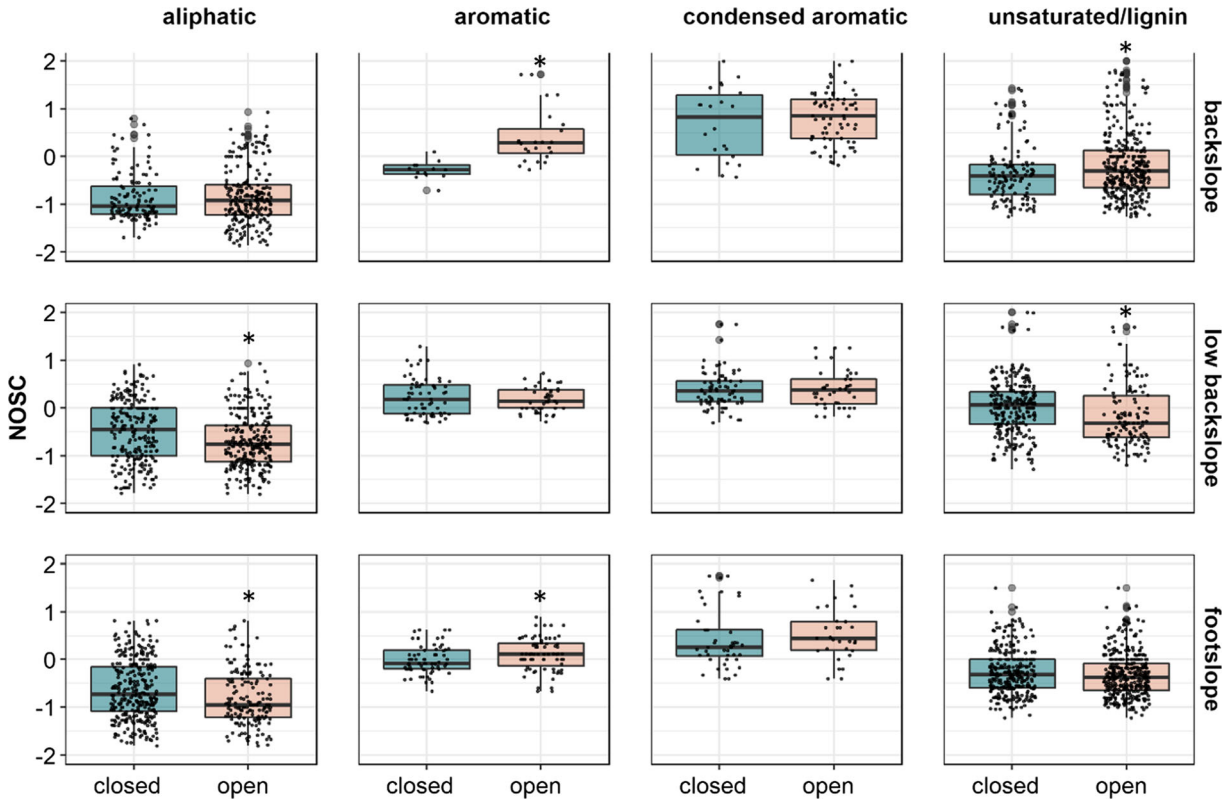

FIGURE A7 Nominal oxidation state of unique compounds (NOSC) under open and closed cover by slope position and compound class. Statistical significance was determined at $\alpha = 0.05$. NOSC was higher in aromatic and lignin-like compounds under open cover on the backslope (compared with closed), whereas it was lower in aliphatic and lignin-like compounds under open cover on the low backslope (compared with closed). NOSC was lower in aliphatics and higher in aromatics under open cover on the footslope position